Mediterranean Geoscience Reviews
https://doi.org/10.1007/s42990-023-00104-4

ORIGINAL PAPER

Late Holocene relative sea-level changes and coastal landscape readings in the island group of Mykonos, Delos, and Rheneia (Cyclades, Greece)

Eleni Kolaiti[1,2,3] · **Nikos Mourtzas**[2,3]

Received: 15 March 2023 / Revised: 7 June 2023 / Accepted: 12 June 2023

Abstract
On the schist, gneiss and plutonic rocky coasts of the island group of Mykonos, Delos, and Rheneia, beachrocks are the main geomorphological sea-level indicators. The detailed mapping and depth measuring of the five distinct beachrock generations identified at 22 locations throughout the coast of the island group point to five corresponding sea-level stands at 4.80 ± 0.10 m, 3.70 ± 0.20 m, 2.40 ± 0.25 m, 1.55 ± 0.25 m, and 0.80 ± 0.10 m below mean sea level, during which each generation was formed. The submerged archaeological sea-level markers found on the coast of the three islands, combined with the recalibrated ages of previously published radiocarbon dating of beachrock cements and the dating of the relevant sea-level stands identified on the islands of the northern and central Cyclades, led to the dating of the Late Holocene relative sea-level changes along the island group coast. From the Late Neolithic period onward, the sea level has risen at continuously increasing rates, with an average value of 0.76 mm/year. The inferred dated sea-level stands enabled the palaeogeographic reconstruction of the seafront of the ancient city of Delos and the Delos Strait, thus revealing both the coastline evolution over time and navigation of the strait during antiquity.

Keywords Sea-level change · Beachrock · Palaeogeography · Ancient Delos · Mykonos · Cyclades

1 Introduction

The island group of Mykonos, Delos, and Rheneia (henceforth referred to as "M–D–R") is located on the SE margin of the northern Cyclades and consists of three islands and seven rocky islets (Fig. 1). It is characterised by continuous human occupation since the sixth millennium BC (Sampson 2018). At the end of the Last Glacial Maximum (~ 20 ka), M–D–R, along with the adjacent islands of the Cycladic archipelago to the north and south of it, constituted a huge island in the middle of the Aegean, occupying an area of about 6800 km^2 (Fig. 2a). At ~ 12 ka, when the sea level rose by about 50 m, a large part of the central Aegean flooded, with M–D–R now constituting a single island of an area of some 270 km^2 (Lambeck 1995, 1996; Lambeck and Purcell 2005) (Fig. 2b). Regarding the Middle and Late Holocene coastal changes and their impact on the coastal communities of the Cycladic archipelago, several geological, archaeological and geoarchaeological approaches have been presented since the early twentieth century, some of these focused on the seafront of the ancient city of Delos and its harbours (Négris 1904; Cayeux 1907; Bernier and Dalongeville 1988; Dûchene and Fraisse 2001; Desruelles et al. 2004, 2007, 2009; Dalongeville et al. 2007; Mourtzas 2012; Zarmakoupi 2015, 2018; Zarmakoupi and Athanasoula 2017, 2018; Nakas 2020).

The first of these was by Négris (1904), who, on the basis of the submerged antiquities along the coast of Delos and Rheneia, estimated a sea-level rise of about 2.50 m during the previous 2000 years. Contrarily, Cayeux (1907), on the basis of his theory of sea-level stability in the Eastern

✉ Eleni Kolaiti
kolaitieleni@gmail.com; Eleni.Kolaiti@nottingham.ac.uk; info@aktes.gr

Nikos Mourtzas
nikosmourtzas@gmail.com; Nikolaos.Mourtzas@nottingham.ac.uk

[1] Institute of Historical Research/National Hellenic Research Foundation (IHR/NHRF), Athens, Greece

[2] Department of Classics and Archaeology, University of Nottingham, Nottingham, UK

[3] Society for the Study of Ancient Coastlines-AKTES NPO, Chalandri, Athens, Greece

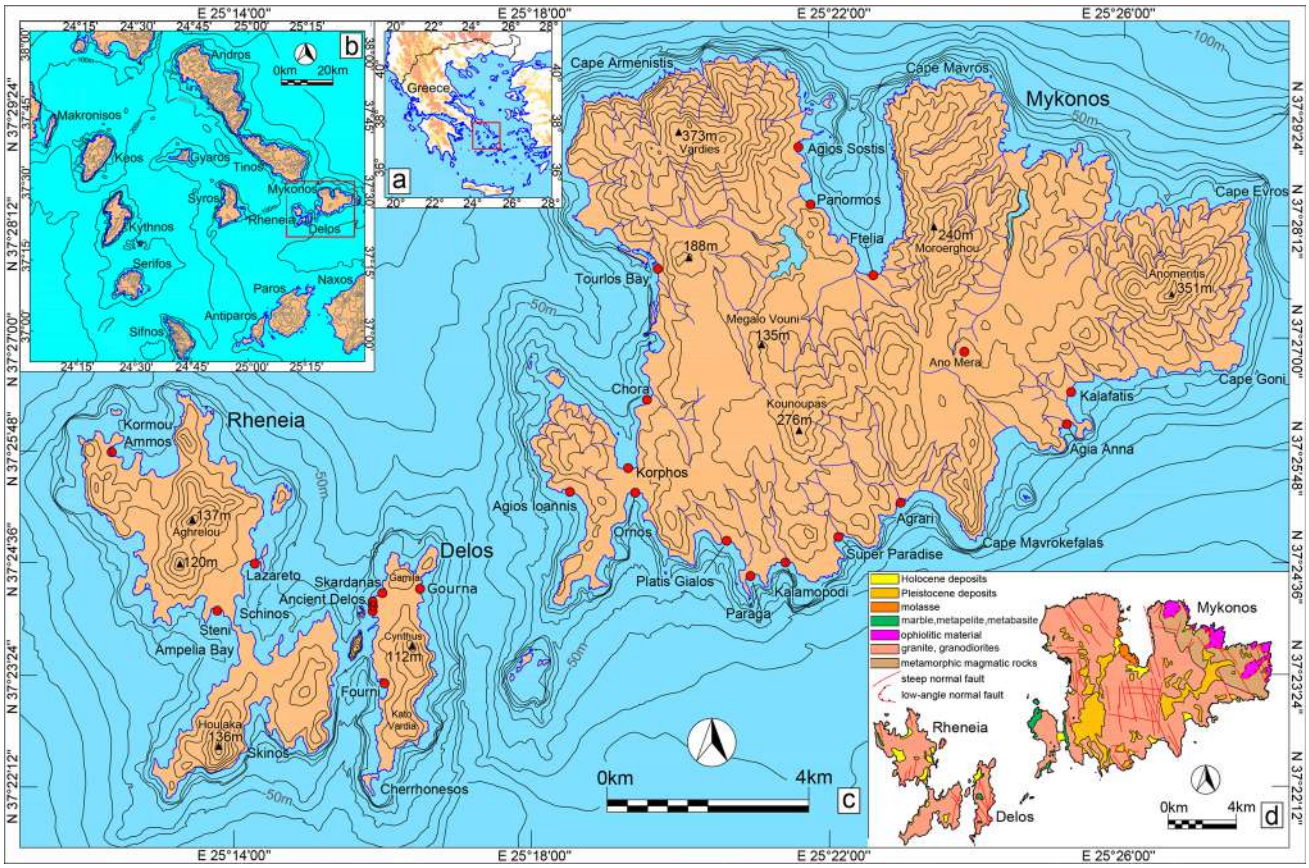

Fig. 1 Location maps of: **a** the northern Cyclades (red square) in Greece, **b** M–D–R (red square) in the northern Cyclades, **c** M–D–R with the locations of the recorded geomorphological and archaeological sea-level indicators (red bullets), and **d** simplified geological map of M–D–R (modified from IGME 2004). M–D–R: the island group of Mykonos–Delos–Rheneia

Mediterranean throughout the historical period, argued that the submerged ancient remains on the coast of Delos were originally constructed under the sea, and attributed the sea transgression to man-made interventions. Desruelles et al. (2009) reconstructed the Late Holocene relative sea-level (henceforth referred to as "rsl") changes in M–D–R using three intertidal, cemented, beachrock generations as sea-level proxies. Surveying seven locations, where the various beachrock generations develop, and establishing their age by a series of ^{14}C AMS dating, they suggested that the sea level was at – 3.60 m (± 0.50 m) around 2000 BC, − 2.50 m (± 0.50 m) around 400 BC and − 1 m (± 0.50 m) around 1000 AD.

This paper aims to shed new light on the magnitude and dating of the rsl changes in M–D–R over the last six millennia. For the purpose of determining the former sea-level stands that correspond to different beachrock generations, a total of 22 locations where beachrocks develop (15 along the coast of Mykonos, four along the coast of Delos, and three along the coast of Rheneia) were surveyed (Fig. 1c), and new rsl data were retrieved. Submerged ancient remains of known age (i.e., seawalls, protective rockfills, boulders, moles, breakwaters, building and castle foundations, tombs, and built bollards), directly related with a former sea level and often incorporated into the beachrock formations, were reassessed in this study as archaeological sea-level indicators. They were further correlated with previously published radiocarbon ages of the beachrock cements, recalibrated anew in this study, allowing the dating of the former sea-level stands to be deduced. This, in turn, led to the palaeogeographic reconstruction of the Delos Strait, at the same time enabling geoarchaeological readings of certain historical reports. Finally, the comparison of the new rsl data from M–D–R with both those from the northern and central Cyclades (Kolaiti and Mourtzas 2020) and the predicted glacio-hydro-isostatic sea-level curve for the central Aegean (Lambeck 1995, 1996; Lambeck and Purcell 2005) allowed us to draw conclusions about the recent tectonic deformation of an area currently characterised by seismic quiescence, amid regions of intense active seismicity.

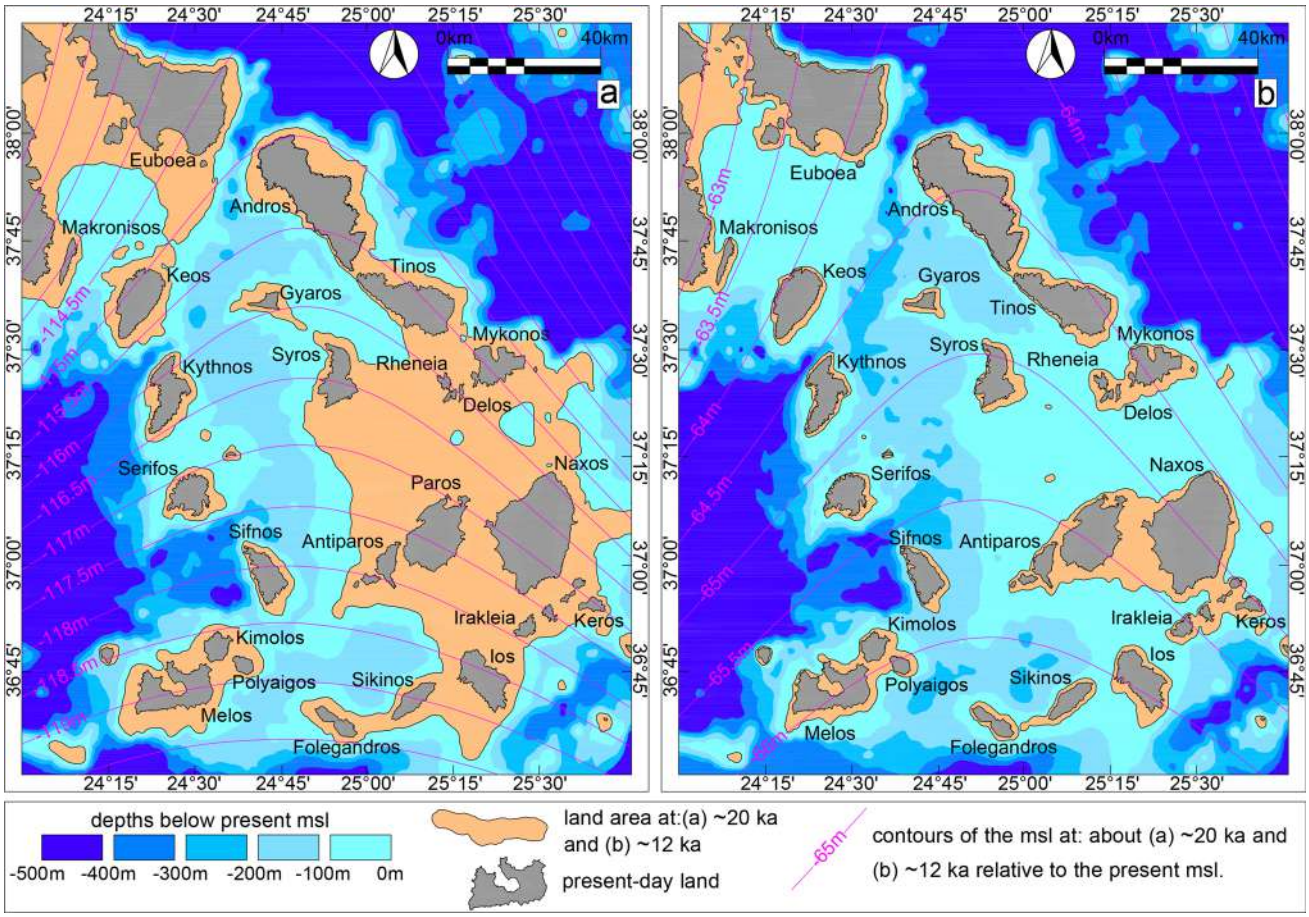

Fig. 2 Predicted relative sea level change for the Cyclades after Lambeck (1995, 1996) and Lambeck and Purcell (2005) at: **a** the Last Glacial Maximum, ~ 20 ka BP and **b** ~ 12 ka BP. The contours represent the position of the mean sea level (msl) at these periods in relation to the present msl

2 Geological setting

Since at least the Early Miocene, the central Aegean region has undergone continental extension, accompanied by the intrusion of granitic plutons and associated detachments (Bröcker and Franz 2005; Rabillard et al. 2018; Jolivet et al. 2021). The morphotectonic evolution of M–D–R begins with the rise and crystallisation of the granodiorite magma and continues with a period of intense erosion and removal of the overlying rocky cover due to the gravity slip of the uppermost units (Karadima 2013).

The island of Mykonos has an area of 106 km^2 and 89 km of coastline. It is of irregular shape with a horizontal (major) axis running 16 km from E to W–SW and a maximum NW–SE breadth of 12 km (Fig. 1c). Hilly terrain prevails, with generally low morphological slopes and limited lowland coastal areas. Low-elevation outcrops are observed in the northern and eastern part of the island, dominated by the summits of Vardies (+ 373 m) and Profitis Ilias Anomeritis (+ 351 m), respectively. The terrain slopes reach up to 80°, with the maximum values observed in the northern and southern coastal parts. In general, flat and even surfaces of land are observed in the central (Ano Mera area) and the western part of the island close to Chora, where the relief is smooth and low. The island does not show a significant hydrographic network, while surface water is drained through a large number of streams of limited length and seasonal runoff. The multifarious coastline mainly follows N–S and E–W directions, with bays deeply penetrating into the land, such as those at Panormos, Korphos, and Ornos (Fig. 1c).

Mykonos and the surrounding islands are dominated by monzogranite, which dates back to around 10–13 Ma (Altherr et al. 1982; Brichau et al. 2008) and which has intruded into the marbles, metapelites, and metabasites of the Cycladic blueschist belt (Brichau et al. 2008) (Fig. 1d). The Cycladic blueschist belt, which consists of a succession of alpine nappes, is a composite unit with a significant component of metabasic rocks included in the metapelites and marbles (Blake et al. 1981; Avigad and Garfunkel

1991; Keiter et al. 2004; Jolivet et al. 2010). It was formed in the footwall of the North Cycladic Detachment System (Jolivet et al. 2010). In Mykonos, the Upper Cycladic Nappe is essentially composed of ophiolitic material (serpentinite, gabbros, and basalt) and high-temperature gneiss and amphibolite of Late Cretaceous metamorphic ages (Maluski et al. 1987; Jolivet et al. 2010). The granite is a kilometer-scale laccolith intruded the micaschists at the top of the migmatitic gneisses of the basement (Faure et al. 1991; Lucas 1999) and crops out only in the SW part of Mykonos and the islands of Delos and Rheneia (Lecomte et al. 2010). The granite is tectonically overlaid by a sequence of coarse-grained detrital Oligo-Miocene (Durr and Altherr 1979) molassic sediments with small slices of Permo-Triassic carbonate, located along the western coast of Panormos Bay (Fig. 1d). The contact between the granite and the overlying molasses is a low-angle normal fault (Avigad et al. 1998). The granites are deformed by the activity of the Livada and Mykonos detachments, which are well exposed on the NE side of Mykonos (Cape Evros) and along the western shore of Panormos Bay (Faure et al. 1991; Lee and Lister 1992; Avigad et al. 1998; Skarpelis 2002). Panormos Bay corresponds to a young N–S trending graben, which cuts through the granite and the metabasites (Lecomte et al. 2010) (Fig. 1d).

Delos is an elongate island, with a maximum N–S length of 5 km, a width of 1.30 km, an area of 6.85 km^2, and 14.20 km of coastline. A central hill range, flanked by short, steep E–W slopes, and interrupted by small plains, runs through the entire length of the island. Its highest point is Mount Cynthus (+ 112 m) in the middle of the island, while Gamila Hill in the northern part and the Kato Vardia low ridge in the southern part reach + 53 m and + 82 m above sea level, respectively. The coast of Delos is steep, forming narrow peninsulas in the northern and southern extremities of the island, and small bays, such as Gourna Bay in the NE part, Skardanas Bay in the NW and Fourni Bay in the SW (Fig. 1c). The island mainly consists of granitoid rocks, with common screens of metamorphosed psammitic schist, marble and amphibolite (Altherr et al. 1982; Pe-Piper et al. 2002) (Fig. 1d). Foliated granodiorite is the principal rock type in the northern part of the island, and megacrystic granodiorite in the central part, while medium-grained granodiorite and granite with abundant enclaves are predominant in the southern part (Pe-Piper et al. 2002). Several shear zones crossing the island separate these rock types and consist of thin screens of metasedimentary rocks and parallel sheets of strained plutonic rocks striking ENE (Pe-Piper et al. 2002).

Rheneia and Delos are separated by a narrow sea channel—the Delos Strait, less than 1 km wide—with two rocky islets between them: Mikros (Little) Rheumatiaris to the north and Megalos (Great) Rheumatiaris further to the south (Fig. 1c).

The island of Rheneia has an area of 13.90 km^2 and 43 km of coastline. Essentially, it consists of two sections connected by a narrow isthmus. The Aghrelou and Houlaka Hills (+ 137 m each) dominate the north and south parts of the island, respectively. The multifarious coastline shapes successive bays, namely those of Kormou Ammos on the northern coast and Skinos on the south coast, as well as Schino to the east and Ampelia to the west of the isthmus, respectively (Fig. 1c). Strongly foliated granites and granodiorites occupy almost the entire island (Lecomte et al. 2010), with only a relic of white, coarse-grained, marble of the Atticocycladic complex on the NW coast (Fig. 1d).

Located between the two recently thinned regions of the North Aegean and the Cretan Sea, the Cyclades domain with an average crustal thickness of 25 km moved as a rigid block towards the South and does not seem to have accommodated any additional extension since the Late Miocene period. Strain rates and GPS velocities in the Cyclades show a relative motion towards SW at a rate of 33–34 mm/yr during the Holocene period (Le Pichon et al. 1995; Kahle et al. 1998; Kreemer and Chamot-Rooke 2004) and scarce and scattered seismicity (Engdahl et al. 1998).

A large portion of the seismic activity within the upper crust is associated with the presence of islands representing horst structures that were generated during the major Oligocene extensional phase. In contrast, the central part of the Cycladic metamorphic core, which today represents the major part of the Cyclades insular group, remains aseismic (Bohnhoff et al. 2006). Lykousis (2009) noted continuous and gradual subsidence of the Aegean margins during the last 400 kyr. The lowest subsidence values (0.34–0.60 mm/year) are related to the low tectonic and seismic activity of the Cyclades plateau, with a gradual decrease in the intensity of the extensional tectonic regime and a decreased isostatic rebound after the Early Pleistocene compressional phase in the Aegean domain (Lykousis 2009). The highest seismic activity was identified along the SW–NE-striking Santorini–Amorgos zone (Papadopoulos and Pavlides 1992; Papazachos et al. 2000; Okal et al. 2009).

3 Beachrocks as indicators of the rsl change

Beachrocks constitute the main geomorphological sea-level indicators along the schist, gneiss, and plutonic rocky coasts of M–D–R, where other coastal geomorphs are absent (e.g., tidal notches: typical of carbonate rocks).

Beachrocks are formed along the shoreline within the intertidal zone, under complex physicochemical (e.g., Ginsburg 1953; Taylor and Illing 1969; Moore 1973; Hanor 1978; Meyers 1987) and biological (e.g., Webb et al. 1999; Neumeier 1999) cementation processes. They consist of coastal sediments, such as sand, gravels, pebbles, cobbles,

and other coarse materials of both clastic and biogenic origin, usually cemented with calcium carbonate, high/low magnesian calcite, and aragonite. It is generally accepted that beachrock lithification takes place in the intertidal zone (e.g., Scholle and Ulmer-Scholle 2003; Vousdoukas et al. 2007; Mauz et al. 2015). In microtidal environments such as this, in the central Aegean where the maximum and mean tidal ranges do not exceed 0.30 m and 0.15 m, respectively (HNHS 2015), the cementation of coastal sediments exceeds the tidal range and expands into the swash, saturated, zone (Gifford 1995; Kolaiti et al. 2017; Kolaiti 2019). The repeated water movement there produces sufficient water circulation in the permeable beach sand, thus creating conditions comparable to those observed at the top of the intertidal zone (Bernier and Dalongeville 1996). Diagenesis is similar in both the intertidal and the swash and backwash zones, and the cementation results are indistinguishable (Bernier and Dalongeville 1996). In the spray zone, which is part of the supratidal zone, water percolates through the sand in the unsaturated zone, and the diagenesis clearly distinguished by the crystal arrangement of the microstalactitic cement at the base of the grains (Taylor and Illing 1969). On the contrary, in the intertidal and phreatic zones, a regularly rimmed, isopachous cement is created around the grains (Longman 1980; Heckel 1983; Bernier and Dalongeville 1996).

The analysis of cements of the various beachrock generations from the northern and central Cycladic archipelago (Andros, Paros, Naxos, Mykonos, Delos, Rheneia, and Sifnos) indicates that everywhere cementation occurs within the intertidal zone (Bernier and Dalongeville 1988; Plomaritis 1999; Alexouli-Livaditi and Livaditis 2004; Desruelles et al. 2009; Karkani et al. 2017).

Previous mineralogical analyses of the M–D–R beachrocks (Bernier and Dalongeville 1988; Desruelles et al. 2004, 2007, 2009; Fouache et al. 2005) have concluded that the beachrocks of Delos and Rheneia are the result of a high-magnesium calcite (HMC) cementation of fine beach sediments of sand, pebbles, cobbles, and shells, and of screes from the adjacent cliffs, ancient architectural elements, artefacts, and potsherds, bound together in the intertidal or even supratidal zone. Two stages of cementation are dominant: the first stage refers to biological cyanobacterian activity that favours the formation of a micritic layer around the grains. Then, acicular HMC crystals grow at the micrite periphery, tending to fill the residual pore space, usually producing a peripheral palissadic and isopachous crystallisation in the intertidal zone, and infrequently a palissadic acicular stalactitic cement in the supratidal zone (Bernier and Dalongeville 1988). The prevailing types of cements observed between the mainly siliceous grains of the M–D–R beachrocks (in some places, a small number of bioclasts and lithoclasts were noted) are diagenetic early intertidal HMC cements, peloidal HMC diagenetic cement, sparitic and microsparitic cements, and micrite, mostly lithified within the intertidal zone, and occasionally non-diagenetic micritic fillings either contemporary or posterior to the lithification in the intertidal zone (Desruelles et al. 2009).

In this study, based on the geomorphological features of beachrocks, their direct or indirect dating, and their current position relative to the coastline, we accept beachrocks as good geomorphological and geoarchaeological indicators of rsl changes, considering that:

- Beachrocks are formed by the cementation of coastal sediments, including anthropogenic deposits, during periods of rsl stability (e.g., Hopley 1986; Strasser et al. 1989; Bernier et al. 1997; Plomaritis 1999; Turner 2005; Vousdoukas et al. 2007; Erginal and Öztürk 2012; Mauz et al. 2015; Avcioğlu et al. 2016).
- Cementation takes place in the coastal zone that is bounded on the seaward end by the mean low water (i.e., the lowermost limit of the intertidal zone) and on the landward end by the uppermost limit of the swash and backwash zone. In exposed microtidal areas, the uppermost limit of the wave uprush is significantly greater than the tidal range (Gifford 1995; Bernier and Dalongeville 1996; Kolaiti et al. 2017).
- Diagenetic cements in the Aegean are usually characterised by HMC, often typical of the marine vadose zone, which extends to the entire swash zone. This implies that diagenesis takes place in environments ranging from the upper marine phreatic to the upper marine vadose zones (e.g., Gifford 1995; Bernier and Dalongeville 1996; Vousdoukas et al. 2007; Desruelles et al. 2009; Vacchi 2012; Kolaiti et al. 2017).
- Different sea-level stands can form distinct beachrock slabs at various elevations, which correspond to different generations of a fossilised palaeoshoreline (e.g., Vousdoukas et al. 2007; Desruelles et al. 2009; Vacchi 2012; Mauz et al. 2015). The loose, unconsolidated, sandy/sandy-gravel sediments laid on the sea bottom between two different beachrock generations represent a period of rsl change (Desruelles et al. 2009; Kolaiti 2019).
- Beachrock slabs dip gently towards the sea, and their slope in line with the initial slope of the beach (e.g., Desruelles et al. 2009). The thickness and lateral extent of beachrocks are dependent on the sediment supply, the width and slope of the beach (accommodation space), and the particular hydrodynamic conditions of the coast (Ginsburg 1953; Shinn 1969; Chivas et al. 1986; Kelletat 1988, 2006; Gischler and Lomando 1997; Ramkumar et al. 2000; Vousdoukas et al. 2007; Mauz et al. 2015). Continuous sediment supply, accumulation, and cementation in the vadose zone can produce a beachrock body thicker than the tidal range (Kolaiti 2019).

- When the cementation process in the intertidal and supratidal zone involves beach deposits that cover an earlier beachrock generation formed during a lower former sea level, a new beachrock generation is then formed, one which partially overlies the previous generation, thus shaping a stepped morphology (Kolaiti 2019).
- The seaward base of a beachrock slab in its well-preserved parts that have not undergone erosion or fragmentation represents the mean low tide of a past sea level (e.g., Mauz et al. 2015). Therefore, to determine the former sea-level stands, the depth/elevation of the seaward base of each beachrock generation can be safely used (Kolaiti 2019). Field observations on the Aegean beachrocks provide excellent evidence of the relationship between the seaward base of beachrocks and the corresponding sea level. Systematic depth measurements made on the seaward end of four dated beachrock generations from 46 locations along the coast of Crete show that the variation in depth does not exceed ± 0.30 m (Mourtzas et al. 2016). The variation in depth of the seaward base of six dated beachrock generations from 49 locations throughout the eastern coast of the Peloponnese stretching for 785 km has proven to be ± 0.20 m (Kolaiti 2019). Similar measurements in five dated beachrock generations from 52 locations along the coast of seven islands of the northern and central Cyclades show a fluctuation not exceeding ± 0.30 m (Kolaiti and Mourtzas 2020; this study).
- The correlation between the depth/elevation of the base of a marine tidal notch and of the seaward base of a beachrock slab, as recorded in many study areas of the Aegean, clearly proves that both geomorphological rsl indicators were formed during the same sea level. Given that the time required for the creation of a marine notch and a beachrock is not the same, we perceive that each one formed at different time intervals but within the same period of rsl stability (Mourtzas et al. 2016; Kolaiti 2019; Kolaiti and Mourtzas 2020). Field observations from the coast of Crete, eastern Peloponnese, and north and central Cyclades (as mentioned above) provide strong evidence of a good agreement between the depths of the seaward base of the beachrock generations and those of the base of the marine tidal notches formed during the same period of rsl stability, showing a maximum difference not exceeding 0.20 m.
- The absolute dating of beachrock cements and fossils or organic material integrated into them by radiocarbon or luminescence dating has not always proved successful for Aegean beachrocks (e.g., Neumeier et al. 2000; Pizarro et al. 2012; Avcioğlu et al. 2016; Karkani et al. 2017; Vacchi et al. 2017). Fossils, organic material, or archaeological remains embedded in a beachrock generation are a *terminus post quem* for the beachrock formation, the latter postdating the embedded material (Kolaiti 2019). Moreover, if there is a good correlation between the depth/elevation of beachrocks dated by absolute dating methods and that of other dated geomorphological or accurate archaeological rsl indicators either formed or in use during the same sea-level stand, then the ages yielded for the beachrocks can be safely accepted (Pirazzoli 2001). This method of approach has proven effective, thus highlighting the importance of beachrocks in rsl reconstructions (e.g., Kolaiti 2019).

Supplementary information is presented in Online Resource, schematically showing the parts of a beachrock slab where depth measurements are collected (Online Resource-Fig. A), the formation process for distinct beachrock generations (Online Resource-Fig. B), the formation process for a beachrock slab in relation with the tidal range during a relatively stable (Online Resource-Fig. C) or rising sea level (Online Resource-Fig. D), and the relation between different beachrock generations and tidal notches formed during the same sea-level stand (Online Resource-Fig. E).

4 Methods

In the present study, a detailed mapping of the distinct beachrock generations throughout the coast of M–D–R was conducted using satellite images (Google Earth Pro, v. 7.3.2), high-resolution orthophotos at a scale of 1:500 (Ktimatologio S.A.), and aerial photogrammetric surveys carried out by an unmanned autonomous vehicle (UAV). The maps produced were updated during snorkelling surveys. Most of the recorded beachrock generations were found to be intact and well-preserved in terms of erosion and fragmentation. The length, width, and thickness, as well as the depth of the top and base of the seaward and landward end of each beachrock generation were measured according to the aforementioned guidelines.

Various ancient coastal constructions dating from the Hellenistic period to Modern Times, although now submerged, clearly relate to the sea level at the time they were in use and are therefore good archaeological rsl indicators for the determination and dating of the former sea-level stands inferred along the coast of M–D–R. Detailed description of the coastal landscape, which entails the recording of the functional features of existing ancient structures, enables a geoarchaeological interpretation of the ancient remains (e.g., Flemming et al. 1973; Lambeck et al. 2004; Antonioli et al. 2007; Auriemma and Solinas 2009; Mourtzas 2012; Anzidei et al. 2013; Mourtzas et al. 2016; Benjamin et al. 2017; Kolaiti and Mourtzas 2020; Kizildağ and Özdaş 2021). Therefore, it is possible to determine both their relationship

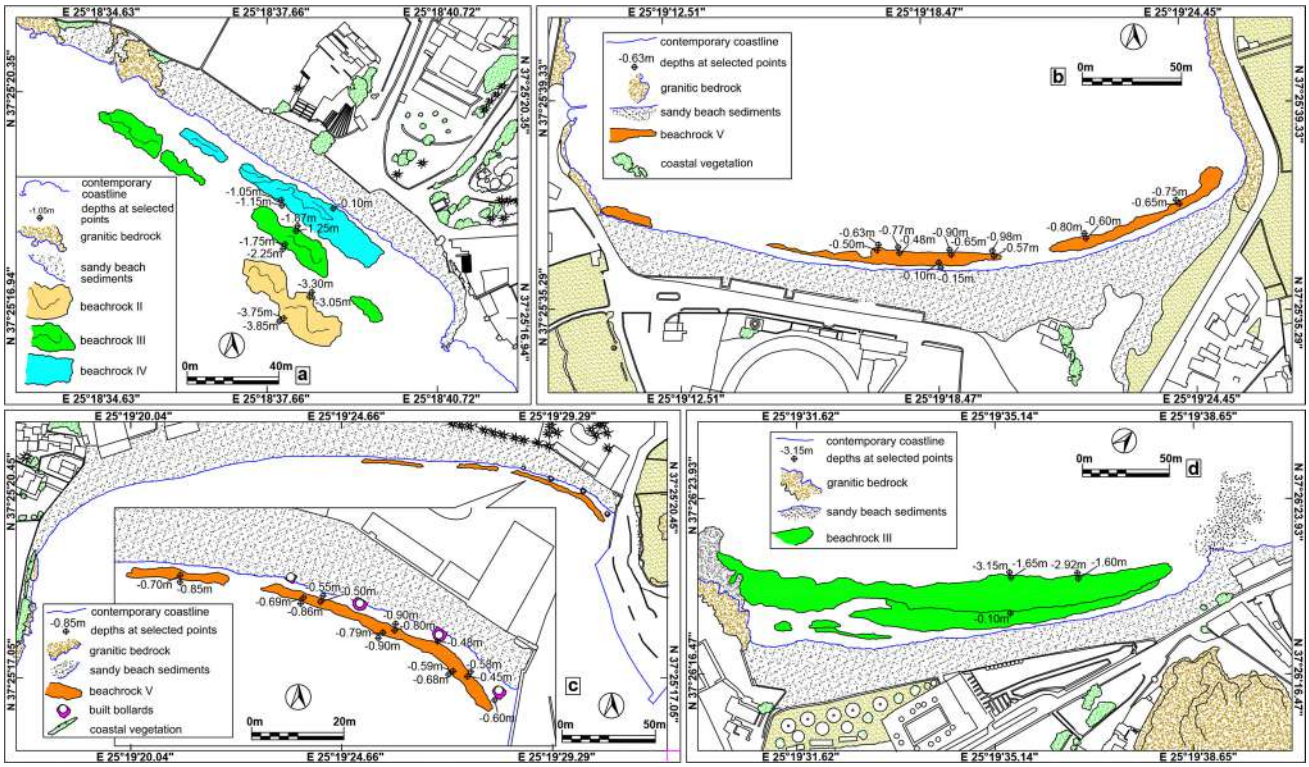

Fig. 3 Detailed mapping and measured depths of the beachrock generations along the coast of Mykonos Island: **a** Agios Ioannis, **b** Korphos, **c** Ornos, and **d** Mykonos Chora

with the sea level during the period they were in use and the length of the intervening period between their construction and their abandonment or destruction (Kolaiti 2019).

All measurements of elevations/depths were collected during calm sea conditions using mechanical methods (namely: a tape measure equipped with a stabilizer system on the measurement surface and a circular metallic ranging rod with conical shoe fitted at the bottom and fully painted with 10 cm-long colour bands in red and white and centimetre division) and recorded using a PVC slate. Measurements in Delos and Rheneia were repeated in two different survey periods (May 1992, June 1993) and were updated in October 2018, along with new measurements that were conducted throughout Mykonos Island. To account for tides, observational data have been reduced for tide values at the time of the surveys with respect to mean sea level, using tidal data from the Hellenic Navy Hydrographic Service for the closest tide-gauge station, in the port of Syros. The effect of atmospheric pressure on the sea level was corrected either using a Dalvey portable barometer (1992–93 surveys) or using the meteorological data for the site at the time of the surveys (2018 survey) (www.meteo.gr). Therefore, all depths and elevations reported herein correspond to depths below mean sea level (bmsl) and elevations above mean sea level (amsl). For the determination of the average depth of each beachrock generation used in the analysis and synthesis of data, we calculated the mean of repeated measurements at the intact and not fragmented parts of the same beachrock generation. The estimated depth uncertainty and resulting error bar were based on the sample standard deviation. The standard error of the mean was also calculated for each data set and was always found to be $< \pm 0.05$ m for a 68% confidence interval and $< \pm 0.10$ m for a 95% confidence interval.

5 Results

5.1 Geomorphological rsl indicators: beachrocks

In this study, a total of 22 locations with beachrock formations throughout the coast of M–D–R were surveyed, the various beachrock generations were recorded and mapped in detail, and the elevations/depths at specific points of each generation, according to the methodology and guidelines presented above, were measured. The locations of the beachrock formations are shown in Fig. 1c, the detailed mapping and the measured elevations/depths for every single study area are illustrated on the detailed location maps of Figs. 3, 4, 5, 6, 7, and 8, and the cross-sections in Figs. 9 and 10. Supplementary information to support field data

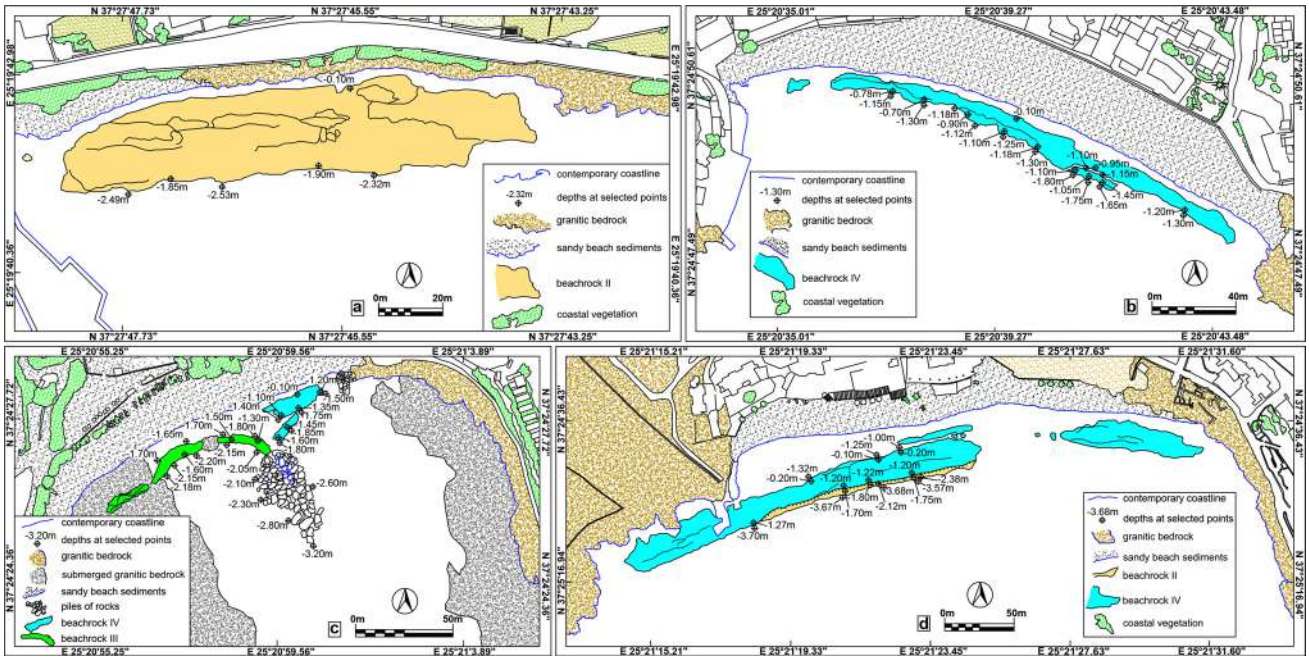

Fig. 4 Detailed mapping and measured depths of the beachrock generations along the coast of Mykonos Island: **a** Tourlos (Mykonos new port), **b** Platis Gialos, **c** Paraga, and **d** Paradise (Kalamopodi)

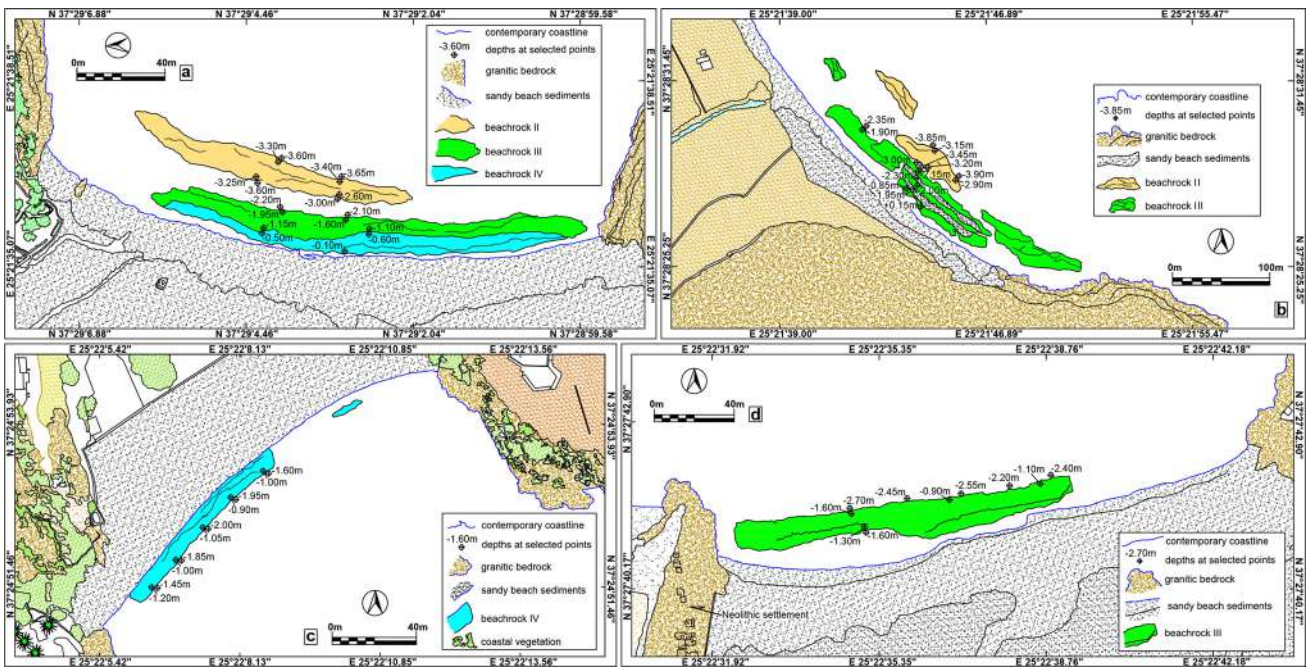

Fig. 5 Detailed mapping and measured depths of the beachrock generations along the coast of Mykonos Island: **a** Agios Sostis, **b** Panormos, **c** Super Paradise (Blindris), and **d** Ftelia

(aerial and underwater views of the beachrock formations throughout the coast of M–D–R) is presented in Online Resource-Figures F and G. The measurements for each beachrock generation and the statistical data analysis are presented in Table 1 and depicted in the four diagrams of Fig. 11, each corresponding to the top and base of the seaward and landward end of each beachrock generation. For the convenience of the reader, the figures for each location

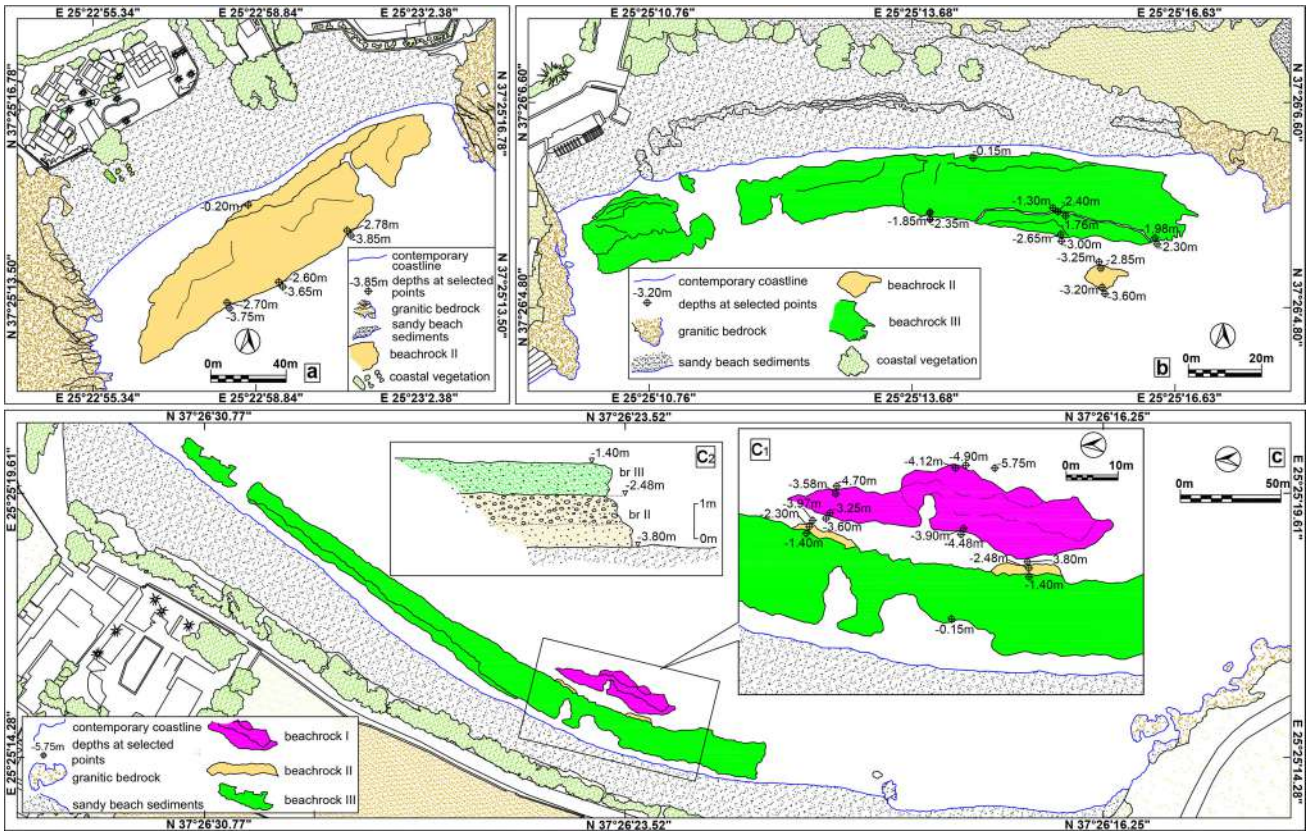

Fig. 6 Detailed mapping and measured depths of the beachrock generations along the coast of Mykonos Island: **a** Agrari, **b** Agia Anna, and **c** Kalafatis (inset c_1: detail of beachrock mapping, inset c_2: beachrock cross-section)

and each beachrock generation are listed in the second column of Table 1. There follows a summary of each beachrock generation, with a brief description of its geomorphic features and explanatory notes on its formation.

5.1.1 Beachrock generation I: 4.80 ± 0.10 m bmsl

The deepest beachrock generation (I) was found submerged only on the coast of Kalafatis, in Mykonos, 36 m from the contemporary shore. The thickness of this beachrock slab ranges from 0.60 m to 1.15 m, its length is 85 m, and its maximum width reaches 17 m.

5.1.2 Beachrock generation II: 3.70 ± 0.20 m bmsl

Beachrock generation II was found in 11 locations: seven along the coast of Mykonos (Agios Ioannis, Paradise, Agrari, Agia Anna, Kalafatis, Panormos, and Agios Sostis), three on the coast of Rheneia (Kormou Ammos, Steni, and Lazareto), and one on the coast of Delos (Fourni). The offshore distance of this generation varies between 38 and 93 m. Its length ranges from 52 to 380 m, its width from 9 to 43 m, and its thickness from 0.10 m to 1.50 m.

5.1.3 Beachrock generation III: 2.40 ± 0.25 m bmsl

Beachrock generation III was identified at 15 locations: nine along the coast of Mykonos (Mykonos Chora, Tourlos, Agios Ioannis, Paraga, Agia Anna, Kalafatis, Ftelia, Panormos, and Agios Sostis), three on the coast of Rheneia (Kormou Ammos, Steni, and Lazareto), and one on the coast of Delos (Ancient Delos seafront). Its length ranges from 80 to 327 m, its width from 7 to 33 m, and its thickness from 0.10 m to 1.45 m. On Kalafatis Beach, beachrock generation III has formed directly upon the previous beachrock slab (II) and overlies it. Besides the characteristic stepped morphology, shaped by their overlapping, they also differ stratigraphically. The lower beachrock slab (II) consists of strongly cemented cobbles (size ≤ 200 mm) and coarse sand, while the upper beachrock (III) comprises strongly cemented medium-to-fine sand (grain size < 0.25 mm) with sparse small (size < 10 mm) pebbles (see insets c_1 and c_2 in Figs. 6c, 9n).

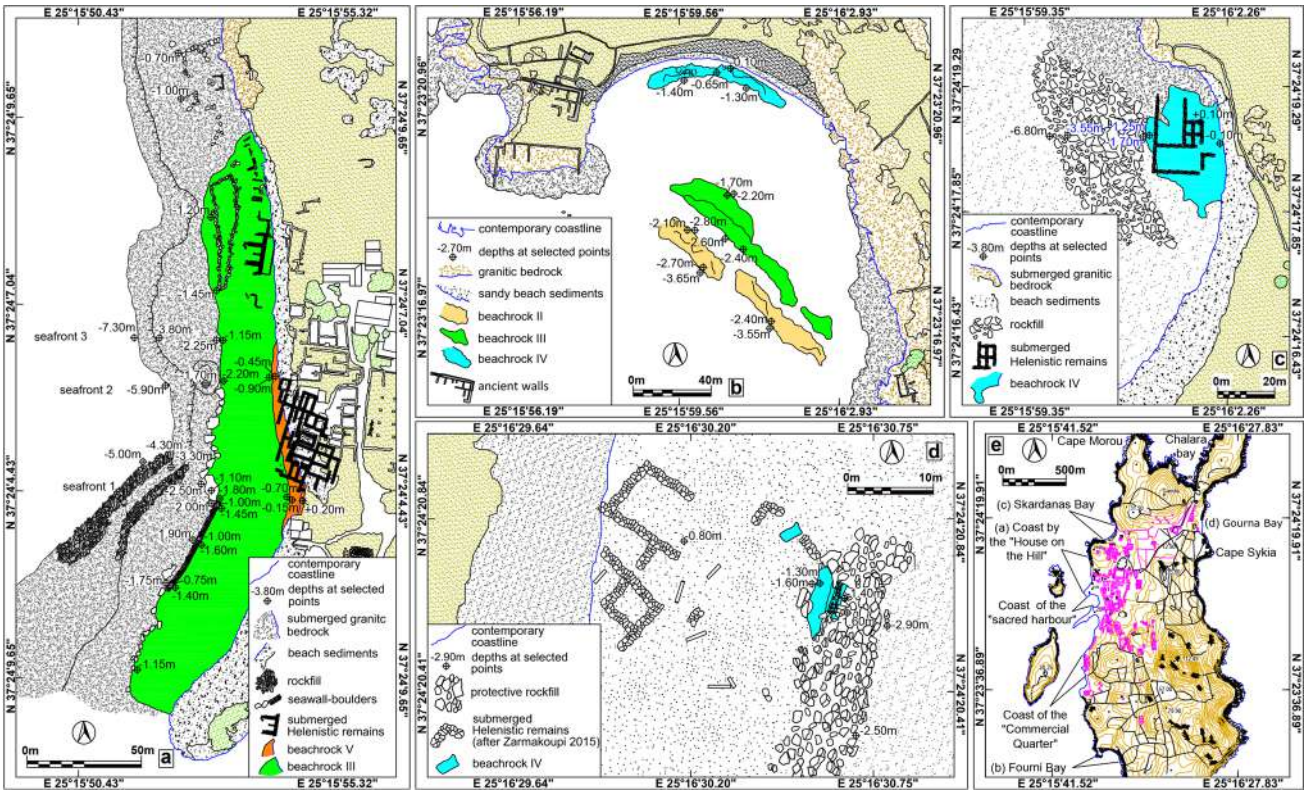

Fig. 7 Detailed mapping and measured depths of the beachrock generations along the coast of Delos Island: **a** Ancient Delos seafront, **b** Fourni, **c** Skardanas Bay, **d** Gourna (Stadium district), and **e** location map of Delos

5.1.4 Beachrock generation IV: 1.55 ± 0.25 m bmsl

Beachrock generation IV was found in 11 locations: six along the coast of Mykonos (Agios Ioannis, Platis Gialos, Paraga, Paradise, Super Paradise, and Agios Sostis), three on the coast of Delos (Skardanas, Gourna, and Fourni), and two on the coast of Rheneia (Kormou Ammos, Steni). Its length ranges from 60 to 430 m, its width from 10 to 29 m, and its thickness from 0.25 m to 1.15 m. On Paradise (Kalamopodi) Beach, beachrock generation IV has also formed directly upon the previous beachrock slab III, overlying it and thus creating a stepped morphology (Figs. 4d, 9n).

5.1.5 Beachrock generation V: 0.80 ± 0.10 m bmsl

The shallowest beachrock identified in M–D–R, beachrock generation V, was found in four locations: two along the coast of Mykonos (Korphos, Ornos), one on the coast of Delos (Ancient Delos seafront), and one on the coast of Rheneia (Kormou Ammos). Its length ranges from 136 to 453 m, its width from 9 to 11 m, and its thickness from 0.20 m to 0.75 m.

5.2 Archaeological rsl markers

5.2.1 Delos Island: the seafront of the ancient city

Situated in the middle of the Cyclades in the Aegean, Delos Island was considered the most sacred of all islands in ancient Greek culture. The first inhabitants settled in Mount Cynthus in the third millennium BC, followed by the Mycenaeans in the lowland in the mid-second millennium BC. The cult of Apollo on Delos begun in the ninth century BC and culminated in the Archaic and Classical periods, rendering Delos a prestigious religious centre. Until the third century BC, the urban area was poorly developed, while in the late third century, many sanctuaries were established for the veneration of almost all the Greek Gods and many foreign deities. In the Hellenistic era, and in particular after 167 BC when it was declared a tax-free port, Delos experienced a population growth with great cosmopolitanism and urban expansion to its port, by now a trading hub for the entire eastern Mediterranean. This prosperity lasted until 88 BC, when Delos was seized by Mithridates' troops and then (69 BC) plundered by the pirates of Athenodorus. The once thriving island fell rapidly into decline, ceased to be a

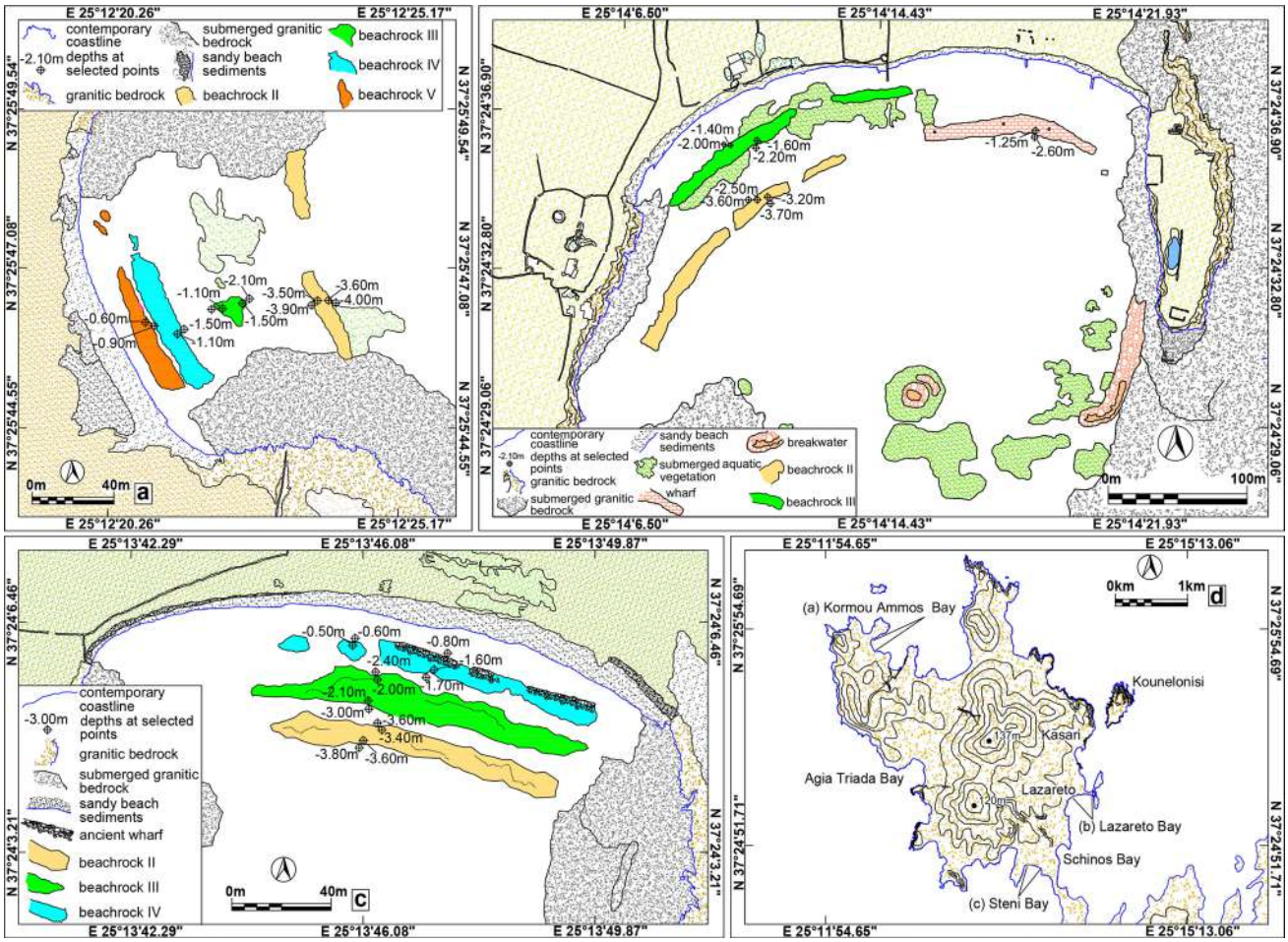

Fig. 8 Detailed mapping and measured depths of the beachrock generations along the coast of Rheneia Island: **a** Kormou Ammos, **b** Lazareto, **c** Steni, and **d** location map of Rheneia

port of call on the sea routes of the time, and was gradually abandoned (Hadjidakis 2003; Efa 2016).

The submerged sea defence structures and buildings all along the seafront of the ancient city of Delos and their correlation with a former sea level have already been presented in detail by Négris (1904) and later by Dalongeville et al. (2007) and Mourtzas (2012).

5.2.2 Delos Island: the coast by the 'House on the Hill'

A seawall, boulders, protective rockfills, and mainly Hellenistic/Late Hellenistic (fourth to first century BC) remains of building foundations, walls, ashlar and stones, and other structures have been integrated into beachrock generation III, running roughly N–S along the coast by the 'House on the Hill' (Figs. 1, 7a,e and 10b1,b2,b3) (Paris 1916; Bernier and Dalongeville 1988; Dûchene and Fraisse 2001; Desruelles et al. 2004, 2007, 2009; Bruneau and Ducat 2005; Dalongeville et al. 2007; Mourtzas 2012; Zarmakoupi 2015). The embedded ancient remains are observed up to a depth of 1.90 m bmsl, while the seaward end of the beachrock is submerged at 2.25 m bmsl (Mourtzas 2012). On the SW seaward side of the beachrock, a built seawall is observed for a length of 45 m, entirely submerged, its top at 0.75–1.00 m bmsl and its base at 1.60–1.90 m bmsl. Within 25 m or so in front of it, towards the open sea, two protective rockfills were placed in two parallel series to protect the coast during a former deeper sea-level stand. Each is around 60 m long, 6 m wide, and 1 m high, peaking at 3.30 m bmsl, and with the sea bottom at the base of the deepest rockfill at 5 m bmsl (Mourtzas 2012) (Fig. 7a).

5.2.3 Delos Island: the coast of the 'Commercial Quarter'

Submerged building foundations, collapsed walls, and numerous potsherds and ashlar blocks are observed in this coastal section, clearly determining the extent of human activity during Hellenistic times (Fig. 7e). The breadth of this area ranges from 9 to 32 m, and the deepest trace of ancient remains reaches 1.70 m bmsl (Mourtzas 2012).

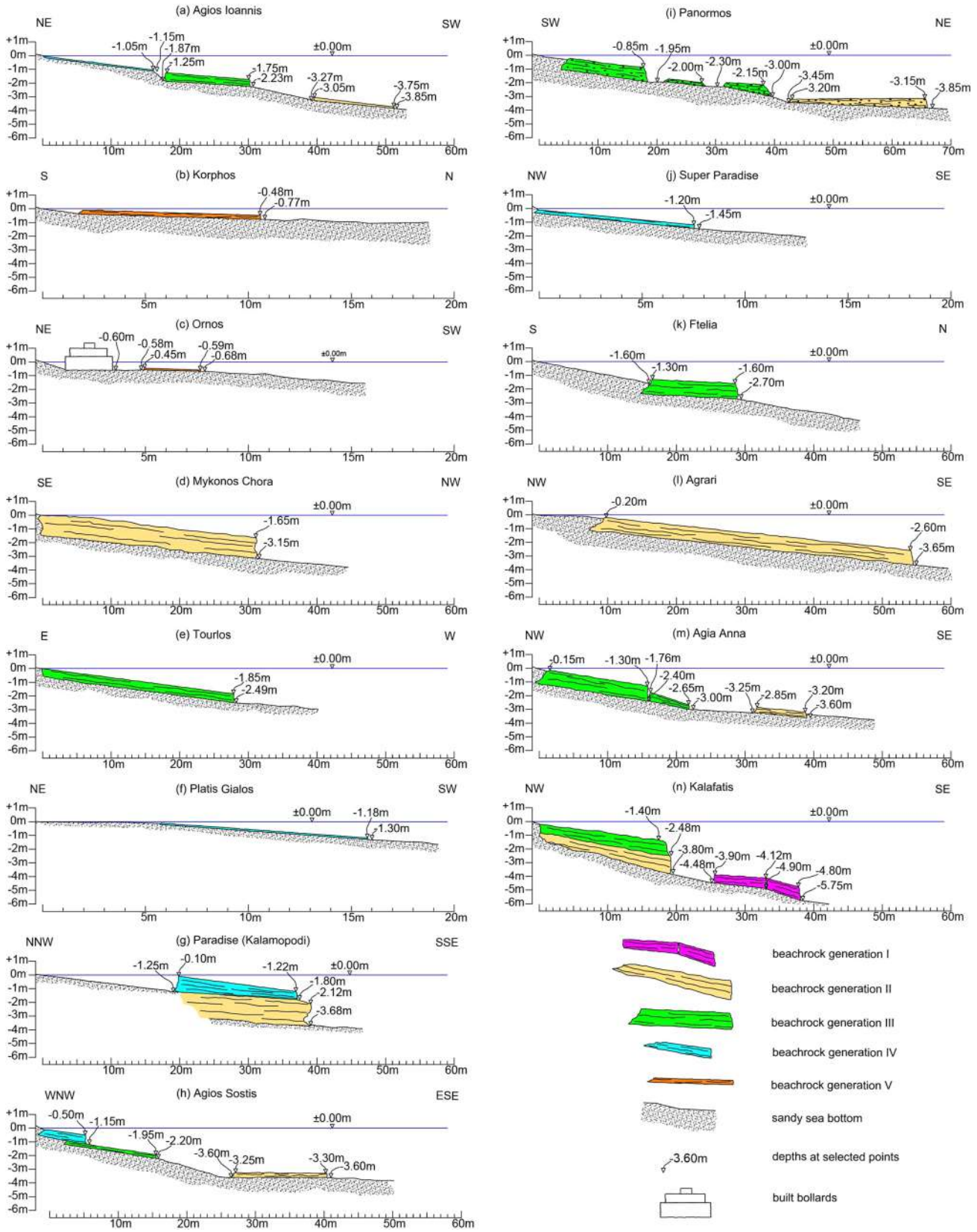

Fig. 9 Cross-sections of the recorded beachrock generations in all the locations surveyed on the coast of Mykonos Island

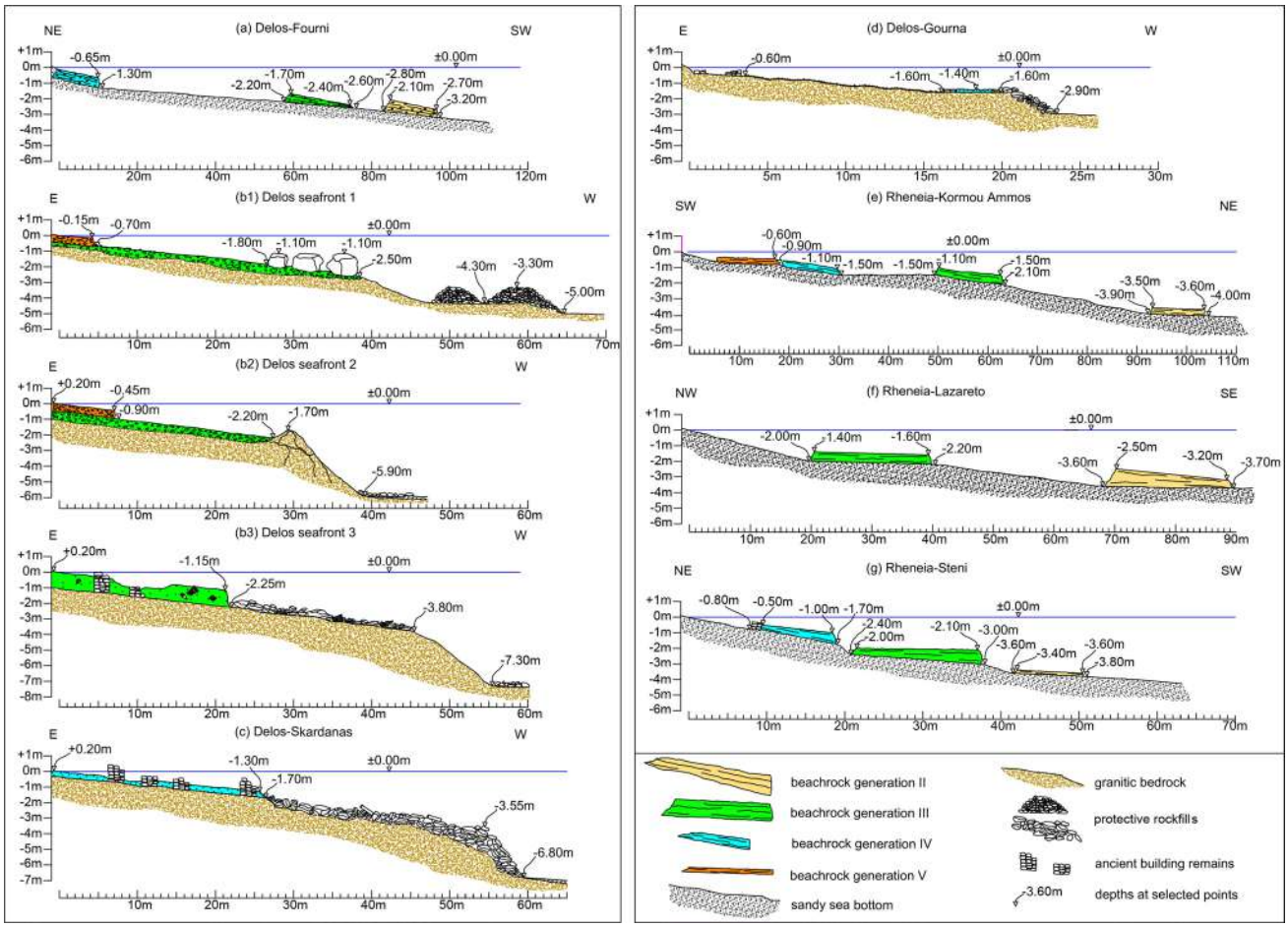

Fig. 10 Cross-sections of the recorded beachrock generations in all the locations surveyed on the coast of Delos and Rheneia Islands

5.2.4 Delos Island: Skardanas Bay

On the NW side of Delos, at the northeasternmost end of the coast of Skardanas Bay (Figs. 1, 7e), the remains of a coastal commercial building have been integrated into beachrock generation IV, close to the shoreline. Many potsherds are scattered up to a depth of 1.25 m bmsl, while the base of the seaward end of this beachrock is at a depth of 1.70 m bmsl (Figs. 7c, 10c).

On the underwater slope in front of the building remains, towards the open sea, a protective rockfill was placed, with its top now at 3.55 m bmsl and its base at the sea bottom at 6.80 m bmsl. It consists of stones and large boulders, among which columns, broken pillars, and pottery fragments can also be found (Figs. 7c, 10c) (Mourtzas 2012).

5.2.5 Delos Island: Gourna Bay (Stadium district)

On the NE side of Delos, in Gourna Bay (coast of the Stadium district) (Figs. 1, 7e), the remains of a large building, beginning at the contemporary shoreline and extending 30 m offshore, were first reported by Papageorgiou-Venetas (1981), who identified them as port facilities. Zarmakoupi (2015) reported clusters of amphorae integrated into the beachrock and parts of the colonnade of the building, and argued that it would serve commercial activities built on the artificially formed shoreline of the time. The depth at the end part of the remains, just in front of the embedded amphorae, is 1.60 m bmsl. At this point, a rockfill begins, comprising large boulders intentionally placed there to protect the building against the waves and which was previously interpreted by Zarmakoupi (2015) as the eastern breakwater of the Stadium district and later by Zarmakoupi and Athanasoula (2018) as a wharf demarcating the easternmost seaward boundary of the Stadium district. Whatever the case, the late Hellenistic submerged remains provide evidence of the rsl change in this area, while the current submerged position of the breakwater, wharf, street, or rockfill, and definitely beachrock generation IV, indicate the magnitude of the rsl rise. The top and base of the protective rockfill are now submerged at 1.60 m and 2.50–2.90 m bmsl (Figs. 7d, 10d).

Table 1 Elevations of the seaward and landward top and base of each beachrock generation of the Mykonos–Delos–Rheneia island group

Location[a]	Figure(s)[b]	Coordinates[c]	Elevation (amsl) / Depth (bmsl)[d] (m)																			
			beachrock generation (V)				beachrock generation (IV)				beachrock generation (III)				beachrock generation (II)				beachrock generation (I)			
			seaward end		landward end		seaward end		landward end		seaward end		landward end		seaward end		landward end		seaward end		landward end	
			top	base	top	base	top	base	top	base	top	base	top	base	top	base	top	base	top	base	top	base
Mykonos Island																						
Mykonos Chora	3d, 9d	37°26'19.86"N 25°19'35.27"E									1.65	3.00±0.10	0.10									
Tourlos (Mykonos new port)	4a, 9e	37°27'48.05"N 25°19'42.34"E									1.85	2.40±0.10	0.10									
Korphos	3b, 9b	37°25'36.01"N 25°19'18.63"E	0.58±0.07	0.80±0.15	0.10	0.15																
Agios Ioannis	3a, 9a	37°25'18.54"N 25°18'38.99"E					1.05	1.15	0.10		1.75	2.25	1.25	1.87	3.75	3.85	3.05	3.30				
Ornos	3c, 9c	37°25'20.49"N 25°19'29.58"E	0.70±0.10	0.80±0.10	0.60±0.15	0.70±0.20																
Platis Gialos	4b, 9f	37°24'50.05"N 25°20'39.28"E					1.00±0.25	1.35±0.25	0.10													
Paraga	4c	37°24'27.85"N 25°20'58.68"E					1.35±0.20	1.65±0.20	0.10		1.50±0.10	2.15±0.10	1.30	1.65±0.15								
Paradise (Kalamopodi)	4d, 9g	37°24'36.14"N 25°21'22.66"E					1.20±0.05	1.75±0.05	0.15±0.05	1.15±0.15					2.25±0.15	3.65±0.05						
Super Paradise (Blindris)	5c, 9j	37°24'53.35"N 25°22'08.30"E					1.05±0.15	1.75±0.25	±0.00													
Agrari	6a, 9l	37°25'15.57"N 25°22'59.37"E													2.70±0.10	3.75±0.10	0.20					
Agia Anna	6b, 9m	37°26'06.15"N 25°25'14.67"E									2.05±0.40	2.50±0.30	0.15		3.20	3.60	2.85	3.25				
Kalafatis	6c, 9n	37°26'26.55"N 25°25'15.66"E									1.40	2.40±0.10	0.15		2.40	3.85±0.10			3.58	4.80±0.10	3.58±0.46	4.04±0.62
Ftelia	5d, 9k	37°27'40.68"N 25°22'35.39"E									1.20±0.35	2.45±0.20	1.30	1.60								
Panormos	5b, 9i	37°28'26.04"N 25°21'45.16"E									2.00	2.30	+0.15 amsl		3.05	3.85	3.20	3.45				
Agios Sostis	5a, 9h	37°29'02.86"N 25°21'35.05"E					0.50	1.15	0.10		1.78±0.25	2.15±0.05	1.10		3.40	3.65	2.90±0.40	3.30±0.30				
Delos Island																						
Ancient Delos seafront 1	7a,e, $10b_1$	37°24'04.52"N 25°15'54.53"E	0.15	0.70	+0.20 amsl						1.80	2.50	0.80±0.10									
Ancient Delos seafront 2	7a,e, $10b_2$	37°24'06.74"N 25°15'54.11"E	0.45	0.90							2.20		±0.00									
Ancient Delos seafront 3	7a,e, $10b_3$	37°24'06.12"N 25°15'54.17"E									1.15	2.25										
Skardanas	7c,e, 10c	37°24'18.80"N 25°16'02.19"E					1.25	1.70	0.10													
Gourna (Stadium district)	7d,e, 10d	37°24'20.87"N 25°16'29.86"E					1.40	1.60	1.30	1.60												
Fourni	7b,e, 10a	37°23'21.76"N 25°16'00.72"E					0.65	1.35±0.05	0.10		2.40	2.60	1.70	2.20	2.55±0.15	3.60±0.05	2.10	2.80				
Rheneia Island																						
Kormou Ammos	8a,d, 10e	37°25'46.74"N 25°12'19.97"E	0.60	0.90			1.10	1.50			1.50	2.10	1.10	1.50	3.60	4.00	3.50	3.90				
Steni	8c,d, 10g	37°24'06.68"N 25°13'47.05"E					1.60	1.70	0.50	0.60	2.10	3.00	2.00	2.40	3.60	3.80	3.40	3.60				
Lazareto	8b,d, 10f	37°24'36.85"N 25°14'09.43"E									1.60	2.20	1.40	2.00	3.20	3.70	2.50	3.60				
average depth of the seaward base of each beachrock generation bmsl (m)				**0.80±0.10**				**1.55±0.25**				**2.40±0.25**				**3.70±0.20**				**4.80±0.10**		

[a] locations are shown in Fig. 1c

[b] figure(s) number(s), in which the detailed mapping, cross-sections and measured depths of each beachrock generation per island and location are illustrated

[c] geographic coordinates, top: Lat (N°), bottom: Long (E°)

[d] all depths are corrected for tide and pressure at the time of the surveys and correspond to depths below mean sea level (**bmsl**); only two values indicated by a plus sign correspond to elevations above mean sea level (**amsl**). The mean of repeated measurements in the same beachrock generation at each location and at different locations from the island group of Mykonos-Delos-Rheneia is calculated. The estimated depth uncertainty and the resulting error bar are based on the sample standard deviation

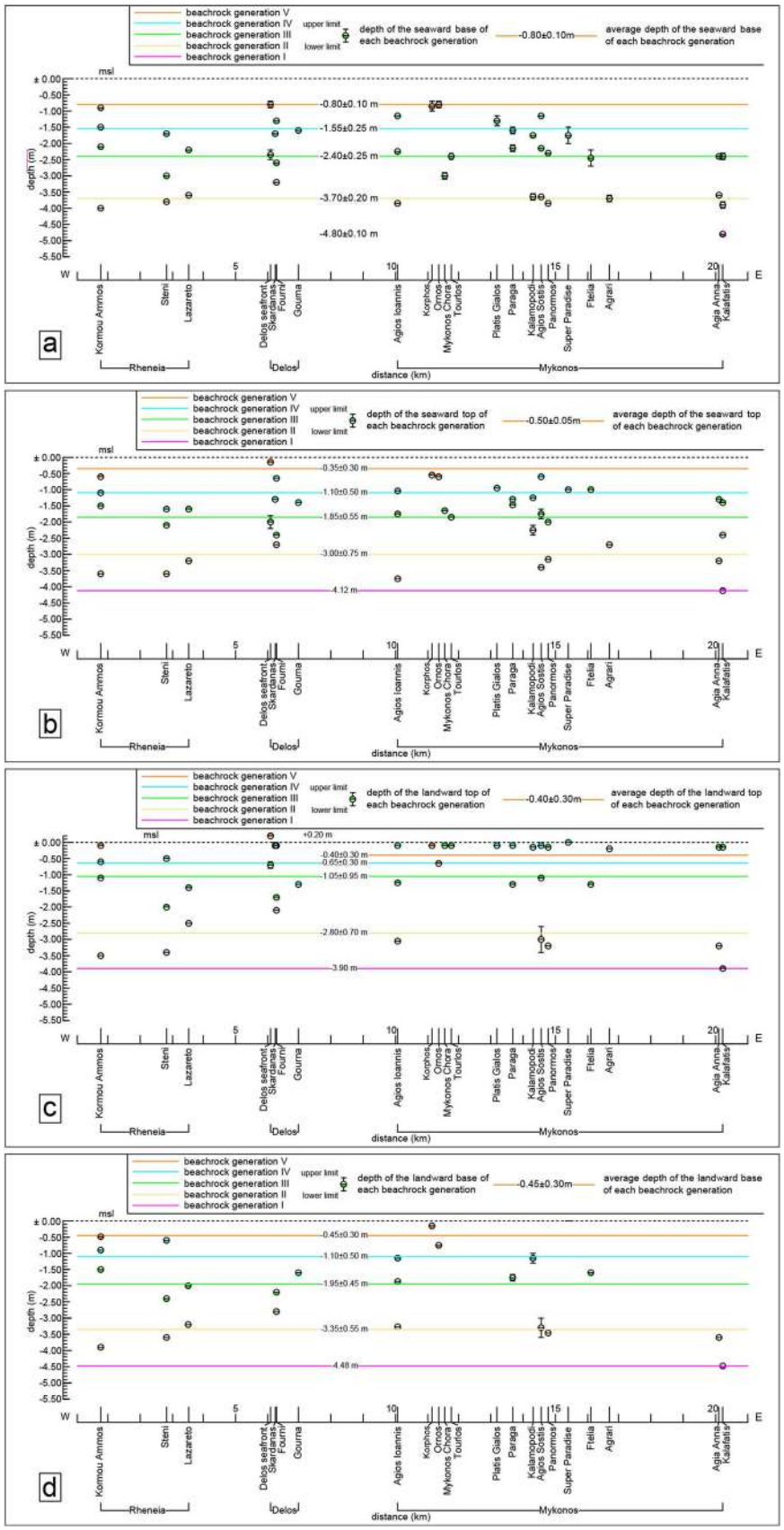

Fig. 11 Average depths of each beachrock generation recorded along the coast of Mykonos, Delos and Rheneia Islands: **a** seaward base, **b** seaward top, **c** landward top, and **d** landward base

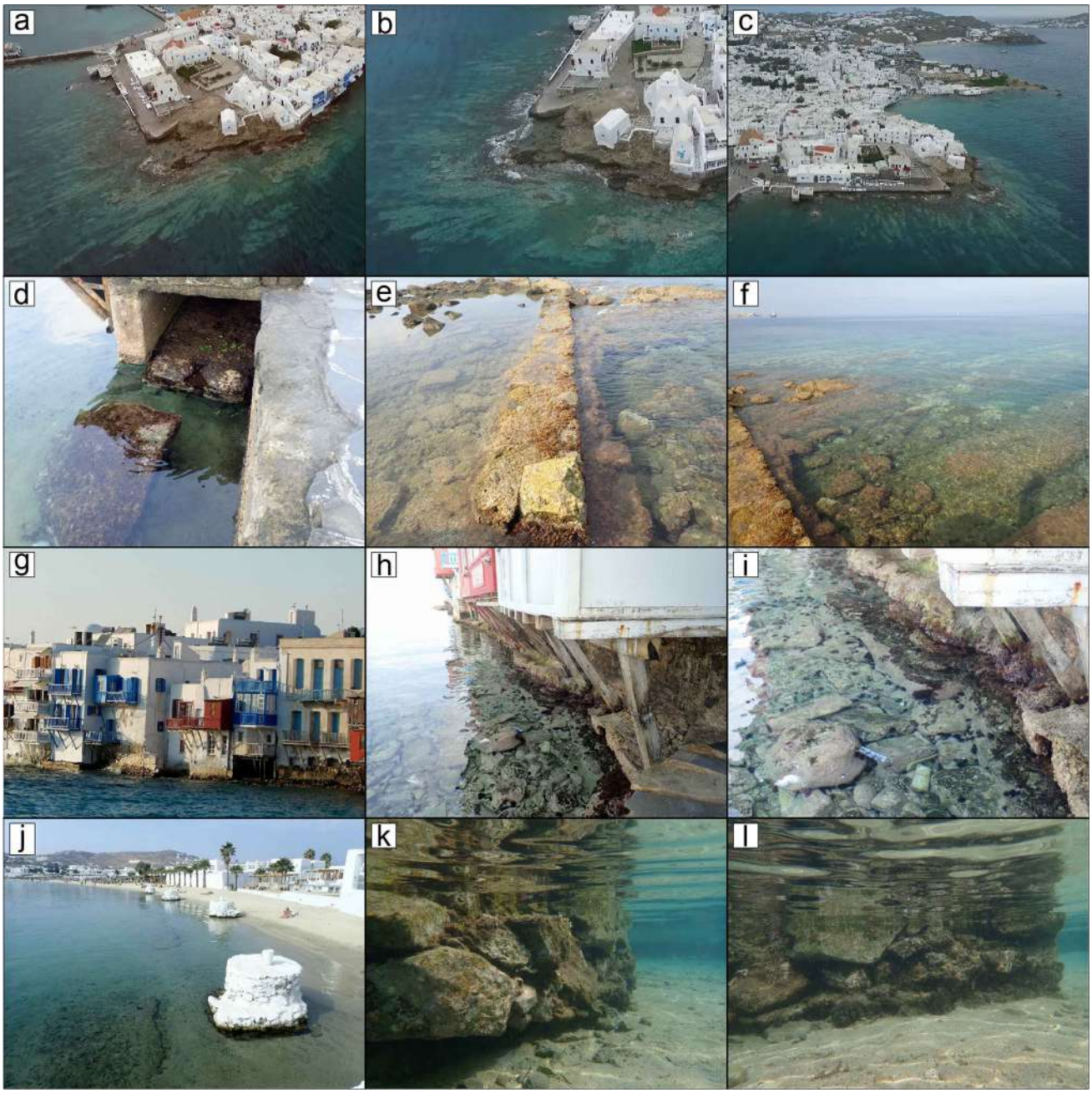

Fig. 12 **a**, **b**, **c** Aerial views of the Kastro neighbourhood founded on a coastal rocky platform, today submerged, on the NW side of Mykonos Chora (retrieved from: https://www.youtube.com/, accessed 9.5.2021). **d**, **e**, **f** Submerged foundations on the south (**d**) and north sides (**e**, **f**) of 'Little Venice' in Mykonos Chora. **g** View from the sea of the coastal buildings of 'Little Venice'. **h** (i) Submerged foundations of the coastal buildings of 'Little Venice'. **j** The built bollards on the Ornos coast in Mykonos, today partly submerged between the landward side of beachrock generation V and the modern coast. **k**, **l** Views of the lower submerged part of the built bollards

5.2.6 Rheneia Island: Lazareto Bay

Rheneia Island (Fig. 1) is located close to Delos, indeed so close as to move Thucydides (3.104.2) to write that, upon its seizure by Polycrates, the tyrant of Samos dedicated Rheneia to Apollo of Delos, tying it to Delos with a chain. The southern part of the island belonged to the territory of ancient Delos, with a sanctuary dedicated to Artemis, and was used as a place of burial and birth of its inhabitants, while land cultivation provided a large part of its revenues to the sanctuary of the Delian Apollo. On the northern part of Rheneia Island was the town, with its cemeteries,

sanctuaries, farmhouses, and various sources of wealth (YPPOA 2020).

On the eastern side of Rheneia, in Lazareto Bay (Figs. 1, 8d), a mole running parallel to and within 40 m from the shore was first reported, surveyed and measured by Négris (1904) and republished later by Dalongeville et al. (2007), who added two underwater views of it. In fact, the mole had been constructed as a continuation of beachrock generations II and III towards the east, following the configuration of the coast of that time (Fig. 8b). According to Négris (1904), the three seaward sides of the mole are vertical, shaped by slabs placed in courses, and elaborated only on their external side. The top of the mole is now at a depth of 1.25 m bmsl and the maximum depth of its base is at 2.60 m bmsl. Four, elongate stone blocks were fixed vertically to the mole. Only two of these are still in place, while the other two have collapsed and been displaced. They are about 3.70 m long, 1.60 m wide, and 0.70 m thick. One of the still-fixed blocks, roughly cylindrical in shape, protruded from the sea about 1 m. Négris (1904) suggested that the structure was a Roman wharf built on land along the shore of the time for the loading and unloading of ships, and that the vertical blocks were bollards for the mooring of vessels.

On the eastern side of Lazareto Bay, there is a rubble mound breakwater; starting from the edge of the small promontory, this develops towards the south (Fig. 8b). Located on the same side of the bay as the wharf and opposite it, the breakwater most likely protected it from the S, SE winds, and waves. Some 100 m to the west of the end of the breakwater, a submerged pile of stones may have served as a lighthouse or a signal post for ships, when the Lazareto harbourworks were in use. Négris (1904) also reported submerged remains of walls of a building near the protection mole to the east, which was made of strongly cemented stones, and other submerged constructions in the southern part of Rheneia, probably belonging to either dwellings or tombs.

5.2.7 Mykonos Island: the Kastro of Chora

The Kastro neighbourhood in the northwestern section of Chora of Mykonos was built on a rough flat-topped rock (+ 10 m) (Fig. 12a, b, c). Archaeological findings provide evidence that the area was continuously in use since the Neolithic era (Konioti 2019; Pelekis 2019). The medieval castle (Kastro) was constructed in the early days of the Duchy of the Archipelago, more precisely, after the Fourth Crusade, when the Ghisi brothers took possession of Mykonos in 1207 (Konioti 2019). After 1537, during the period of Ottoman rule, there had been a fortified, walled-in, densely built seaside town of about 1000–1500 people concentrated in an area of 7500 m^2. The walls had three or four defence towers and three entrances, very few remains of which survive today. One of the entrances, the seashore entrance joining the Kastro with the harbour, was demolished in 1900; however, there is historic iconography of Kastro dating back to the fourteenth century AD (Pelekis 2019). The waterfront remains of the foundations of the walls and parts of their masonry are situated at the NW end of Chora, on both sides of the 'Little Venice" district, which once defined one of the four sides of the fortified Kastro. The northernmost coastal section of the Kastro settlement, part of which was unearthed by the recent archaeological excavations (Konioti 2019), rests on an even rocky platform, mostly artificially formed as indicated by the traces of cuttings that are still preserved there (Fig. 12f). The rocky platform extends for 40 m offshore and is sinking under the sea at a maximum depth of 1.50 m bmsl. Its seaward edge is demarcated by a steep underwater slope. The foundations and parts of the castle superstructure, once built on dry land, are now submerged at 0.70 m to 1.10 m bmsl (Fig. 12e, f). At the south end of the 'Little Venice' district, the preserved foundations of the Venetian castle are now submerged at 0.75 m bmsl (Fig. 12d).

5.2.8 Mykonos Island: 'Little Venice'

Throughout the eighteenth and nineteenth centuries, due to its geographic position, Mykonos was an important supply port for merchant ships sailing in the Aegean. The mid-eighteenth century, in the area south of Kastro, saw the creation of the Alefkandra neighbourhood, where wealthy merchants and captains built their residences along the waterfront, with windows and doors facing the open sea and wooden balconies overhanging the sea (Fig. 12g). This picturesque district is widely known by the toponym 'Little Venice'. The thick walls of the houses were made of stones plastered with lime (Schmidt 2006), the foundations having been made on dry land either directly on the flattened rock (mainly at the northern end of the district), or by utilising the older foundations of the castle (as on its southern side). Although it is hard to distinguish the older from the newer part of the foundations, the waterfront stairs of the houses today submerged provide evidence of submersion of the newer foundations of about 0.40 m to 0.60 m bmsl (Fig. 12h,i).

5.2.9 Mykonos Island: built bollards on the Ornos coast

All along the easternmost part of Ornos Beach, four cylindrical structures 1.70–2 m in diameter were constructed about 17 m distant each other (Figs. 1, 3c, 9c, 12j). They are made

of rough stones, bound together with mortar. According to local fishermen, the bollards were most probably built in the early twentieth century, but this is not confirmed by written sources. The lower part of the built bollards is now submerged at a depth of 0.48 m to 0.60 m bmsl (Fig. 12k, l). What is more important, the built bollards are located just behind the landward end of beachrock generation V, which demarcates the shoreline of the period when the bollards were in use.

5.3 Recalibrated ^{14}C ages of beachrock generations

The conventional ^{14}C ages of the M–D–R beachrocks were calibrated by Desruelles et al. (2009) using the curve of Hughen et al. (2004) and corrected for the local marine reservoir effect with a $\Delta R = -393 \pm 40$ year. This value was suggested by Facorellis and Maniatis (2002), exclusively for the first half of the fifth millennium BC in the case of the Neolithic settlement of Ftelia (Mykonos). In this study, we recalibrated the conventional ^{14}C ages obtained by Desruelles et al. (2009) using the Marine13 curve and Calib 7.1 software (Reimer et al. 2013; Stuiver et al. 2018) and we corrected these for the local marine reservoir effect with a mean $\Delta R = 58 \pm 85$ yr, as suggested by Reimer and McCormac (2002) for the Mediterranean Sea. It should be noted that correction for the local marine reservoir effect using the different ΔR values suggested by Reimer and McCormac (2002) for the Aegean Sea and Piraeus yielded (2σ) ages not significantly differentiated than those suggested in this study and definitely falling within the same chronological range. The new radiocarbon ages are expressed in calibrated years BP and BC at 68% probability (1σ) and 95% probability (2σ) and are summarised in Table 2. Along general lines, the new recalibrated ages are almost all younger than the previously calibrated ages.

Although in the plutonic–volcanic geological regime of M–D–R, the sources of carbonate pollution are limited, radiocarbon dating on the 'total sample' proved problematic, providing heterogeneous results some of which deviated from the age/depth trend line. Desruelles et al. (2009) attributed the discrepancies in ages to turbulent sediment transit, mineralogical composition, cement ageing by carbonate clasts and micritic fillings, and the presence of non-diagenetic micrite in the internal sediments, which rather tends to give older ages, as well as the embedded archaeological remains that give very recent ages in comparison with the overall tendency. In this regard, we have excluded from our reassessment, as did Desruelles et al. (2009), those ages that do not conform to the general model of beachrock formation: the deeper the beachrock generation, the older the dating. However, more importantly, both the original and recalibrated ages of beachrock generations II, III, IV, and V (Table 2), as categorised according to the depths determined in this study, are spread over a wide chronological range (e.g., 3.3 ka for beachrock II, 1.3 ka for beachrock III, and 1.2 ka for beachrock IV). This necessitates verification of the radiometric ages by other methods, as strongly recommended by Pirazzoli (2001). In this regard, we consider in our interpretation those values that are in agreement with the indirect geoarchaeological dating, that is the chronological range of the archaeological rsl indicators, which were in use during the respective periods of rsl stability in which the beachrock generations were formed. The two extremes of the chronological range for beachrock II (3.70 ± 0.20 m bmsl) are 1972 BC and 12 BC and for beachrock III (2.40 ± 0.25 m bmsl) 73 BC and 1272 AD. A certain age for beachrock generation IV (1.55 ± 0.25 m bmsl) is 1605–1615 AD. The remaining beachrock generations (I, V) are indirectly dated, solely on the basis of geoarchaeological criteria.

6 Discussion

6.1 Rsl reconstruction along the coast of M–D–R

The identified mean sea-level stands in M–D–R and those of the northern and central Cyclades are remarkably consistent in terms of depth and are both illustrated in the time-depth diagram of Fig. 13.

The deepest sea level (I) is determined by the deepest beachrock generation (I) found on Kalafatis coast at 4.80 ± 0.10 m bmsl (Figs. 11a, 13, Table 1). The deepest sea-level stand determined for the northern and central Cyclades at the same depth (5.00 ± 0.10 m bmsl) as that of Kalafatis is dated back to between the Late Neolithic and the end of the Early Bronze Age (4300 BC to 2000 BC), on the basis of good archaeological rsl markers from Keos Island and Paros-Antiparos Strait (Mourtzas 2010, 2018; Mourtzas and Kolaiti 1998, 2016; Kolaiti and Mourtzas 2020).

The depth of the seaward end of beachrock II recorded throughout M–D–R determines the next sea-level stand (II) at 3.70 ± 0.20 m bmsl (Figs. 11a, 13, Table 1). The protective rockfills in Skardanas Bay (top: 3.55 m bmsl) and on the coast by the 'House on the Hill' (top: 3.30 m bmsl) would have been functional during sea-level stand II. The respective sea-level stand identified in the northern and central Cyclades at 3.60 ± 0.20 m bmsl, based on many archaeological rsl markers, dates back to between the end of the Early Bronze Age (2000 BC) and the end of the late Hellenistic period (ca. 30 BC), and for M–D–R definitely after its destruction by Mithridates in 69 BC (Mendoni and Mourtzas 1990; Mourtzas 2010, 2012; Mourtzas and Kolaiti 1998, 2016; Kolaiti and Mourtzas 2020). The recalibrated ^{14}C ages of the seaward and landward ends of beachrock generation II fall within this chronological range (1972 BC to 12 BC).

Table 2 Radiocarbon ages of the Mykonos–Delos–Rheneia beachrocks, recalibrated and corrected for local marine reservoir effect

Location[a]	Sample code[b]	Sample position[c]	Sample depth[d] (m)	^{14}C age[e] (yr BP)	Calibrated Age (BC/AD)[f]	Recalibrated and reservoir corrected ages (present study)[g]			
						(1σ) cal age ranges (yr BP)	(2σ) cal age ranges (yr BP)	(1σ) cal age ranges (BC/AD)	(2σ) cal age ranges (BC/AD)
Beachrock generation II (3.70 ± 0.20 m bmsl)[h]									
Kalafatis, Mykonos	A22	s.e	3.80	3185 ± 45	1112–964 BC	2785–3024	2722–3163	1075–836 BC	1214–773 BC
Kormou Ammos, Rheneia	E32	s.e	3.60	3815 ± 30	1867–1764 BC	3579–3813	3453–3921	1864–1630 BC	1972–1504 BC
Lazareto, Rheneia	G22	s.e	3.20	2775 ± 30	650–487 BC	2316–2572	2240–2697	623–367 BC	266–260 BC
Agios Ioannis, Mykonos	B31	l.e.[i]	3.50	4860 ± 35	3309–3165 BC	4962–5232	4841–5298	3283–3013 BC	3349–2892 BC
Agios Sostis, Mykonos	C21a	l.e.[j]	3.00	1750 ± 25	628–680 AD	1160–1336	1041–1433	614–790 AD	517–909 AD
Agios Sostis, Mykonos	C21b	l.e.[j]	2.80	3745 ± 30	1770–1665 BC	3473–3709	3382–3831	1760–1524 BC	1882–1433 BC
Steni, Rheneia	F21	l.e.[k]	3.40	2595 ± 30	380–294 BC	2101–2315	1961–2426	366–152 BC	477–12 BC
Beachrock generation III (2.40 ± 0.25 m bmsl)[h]									
Agios Ioannis, Mykonos	B22	s.e	2.20	2265 ± 30	36–123 AD	1693–1913	1574–2022	37–257 AD	73BC-376AD
Steni, Rheneia	F12	s.e	2.10	1380 ± 30	991–1055 AD	762–951	678–1050	999–1188 AD	900–1272 AD
Kormou Ammos, Rheneia	E22	s.e	1.50	2175 ± 30	137–229 AD	1591–1809	1492–1920	141–359 AD	30–458 AD
Lazareto, Rheneia	G12	s.e	2.00	1635 ± 25	710–780 AD	1045–1235	941–1289	715–905 AD	661–1009 AD
Agios Ioannis, Mykonos	B21	l.e.[l]	1.45	2465 ± 45	235–82 BC	1909–2156	1827–2294	207 BC-41 AD	345 BC-123 AD
Fourni, Delos	D21a	l.e.[m]	1.80	1700 ± 30	661–720 AD	1103–1286	985–1363	664–847 AD	587–965 AD
Fourni, Delos	D21b	l.e.[m]	1.70	2545 ± 25	330–228 BC	2048–2277	1919–2337	328–99 BC	388 BC-31 AD
Beachrock generation IV (1.55 ± 0.25 m bmsl)[h]									
Agios Ioannis, Mykonos	B11	s.e	1.25	1775 ± 40	596–672 AD	1173–1361	1062–1479	589–777 AD	471–888 AD
Agios Sostis, Mykonos	C12	s.e	1.30	970 ± 35	1349–1423 AD	462–610	355–662	1340–1488 AD	1605–1615 AD
Kalafatis, Mykonos	A11	m	1.00	1330 ± 35	1032–1122 AD	726–905	649–998	1045–1224 AD	952–1301 AD
Steni, Rheneia	F11	m	1.00	1610 ± 30	723–811 AD	1014–1213	924–1274	737–936 AD	676–1026 AD
Beachrock generation V (0.80 ± 0.10 m bmsl)[h]									
Kormou Ammos, Rheneia	E11	l.e.[n]	0.60	1300 ± 25	1058–1140 AD	707–880	638–957	1070–1243 AD	993–1312 AD

[a]Locations are shown in Fig. 1c

[b]Code of samples as given in Desruelles et al. (2009)

[c]Position of sample in reference to the landward or seaward end of the beachrock slab (s.e.: seaward end, l.e: landward end, m.: in the middle of beachrock). When the sample is taken from the landward end or middle of the beachrock, the depth of the seaward end is also mentioned in the corresponding note (see below, notes i to n)

[d]Depth of sampling (tide corrected) as given in Desruelles et al. (2009)

[e]Conventional ^{14}C ages as published by Desruelles et al. (2009)

[f]The conventional ^{14}C ages were calibrated by Desruelles et al. (2009) using the curve of Hughen et al. (2004) and corrected for local marine reservoir effect with a $\Delta R = -393 \pm 40$ yr, as suggested for the first half of the fifth millenium BC in the case of Ftelia (Mykonos) byFacorellis and Maniatis (2002)

[g]The conventional ^{14}C ages obtained by Desruelles et al. (2009) were recalibrated in the present study using the curve Marine13 and Calib 7.1 software (Reimer et al. 2013; Stuiver et al. 2018) and corrected for local marine reservoir effect with a mean $\Delta R = 58 \pm 85$ yr, as suggested by Reimer and McCormac (2002) for the Mediterranean Sea

[h]Average depth of each beachrock generation assessed in this study through multiple depth measurements on the same beachrock generation recorded in different locations (see Table 1). The values are corrected for tide and pressure at the time of the surveys and corrrespond to depths below mean sea level (bmsl)

[i,j,k,l,m,n]Depths (bmsl) of the seaward end measured by Desruelles et al. (2009): [(i)] 3.80–4.00 m, [(j)] 3.70–4.00 m, [(k)] 3.80 m, [(l)] 2.50 m, [(m)] 2.40 m, [(n)] 0.90 m

Sea-level stand III is evidenced by beachrock generation III at 2.40 ± 0.25 m bmsl (Figs. 11a, 13, Table 1) found in many locations alongside the M–D–R coast. The Hellenistic remains embedded in beachrock III on the seafront of the ancient city are a *terminus post quem* for the beachrock formation, which postdates the collapsed embedded material. Beachrock III was definitely cemented after the Hellenistic coastal buildings had collapsed and been abandoned. Their ruins, along with the sea defence that once protected them (e.g., boulders, rockfills, and seawall, which all are now aligned between the isobaths of 2.00 m and 2.50 m), were located along the then coastline and subject to the cementation process (Fig. 14a). This is compelling evidence of the post-Hellenistic chronology of this sea level. In the central and northern Cyclades (Fig. 13), this change occurred sometime between 30 BC (end of the Hellenistic period) and 41 AD (a chronology reported in a testimony that the ancient harbour of Palaiopolis in West Andros was still in use) (Mourtzas 2007, 2012, 2018; Kolaiti and Mourtzas 2020). It seems that sea level III may have lasted for one millennium or even more: on the one hand, the recalibrated ^{14}C ages of beachrock III fall within these chronologies (73 BC to 1272 AD) and, on the other, the next sea-level stand (IV) has been ascertained as the sea level during the Venetian domination of the Cyclades (thirteenth to sixteenth century AD).

The depth of the seaward end of beachrock IV found all along the M–D–R coast determines the sea-level stand IV at 1.55 ± 0.25 m bmsl (Figs. 11a, 13, Table 1), which as previously mentioned dates to the Venetian domination of the Cyclades (1207 to ca. 1566 AD, with Mykonos being occupied by the Ottomans in 1537). The rock-cut platform, foundations, and parts of the masonry of the Venetian castle in Chora (Mykonos) submerged up to a depth of 1.50 m bmsl suggest that the coastal part of the castle would have been constructed during an equivalent level or even slightly lower than the platform and the foundation level of the castle. The harbourworks in Lazareto Bay could have been functional at this sea level and are therefore associated with the Venetian period of M–D–R, and not dated to Hellenistic or Roman times as Négris (1904) suggested. In order for Négris to justify the functionality of the mole at the minimum sea level he had concluded (2.50 m lower than at present), he assumed that the ships approaching Lazareto Bay for loading and unloading communicated with the wharf by mobile walkways. The vertical stone bollards may have been architectural elements that were integrated into the mole for a secondary use. A similar sea-level stand at 1.50 ± 0.20 m bmsl has been established by many geomorphological rsl indicators throughout the northern and central Cyclades and, based on the indirect dating of archaeological sea-level markers, dates back to the Venetian period (Fig. 13). The shift to the next sea level (V) could be linked with the period between 1649 and 1735, during which a series of strong seismic events and the eruption of the Kolumbo active submarine volcano off the NE coast Santorini in 1650 (Mourtzas 2018; Kolaiti and Mourtzas 2020). The recalibrated radiocarbon age of beachrock IV (1605–1615 AD) fully supports this assumption.

Sea-level stand V at 0.80 ± 0.10 m was determined by beachrock generation V formed on Mykonos and Delos coast (Figs. 11a, 13, Table 1). By correlating it with the depth of the foundations of the coastal buildings in 'Little Venice' and the built bollards in Ornos Bay, it dates to the early nineteenth century. The respective sea level V at 0.90 ± 0.20 m bmsl, established for the entire northern and central Cyclades (Fig. 13), is dated to after the Venetian period and during the Ottoman rule of the Cyclades (sixteenth to nineteenth century). The change to the next sea level stand could be linked to the strong seismic sequence that struck Kythnos Island between 29.4.1891 and 11.5.1891 (Mourtzas 2018; Kolaiti and Mourtzas 2020).

Finally, no evidence of the most recent sea level stand (VI) identified in the northern and central Cyclades at 0.45 ± 0.15 m bmsl (Fig. 13) has so far been found in M–D–R. Sea level VI was determined by the depth of the well-incised marine tidal notches and well-developed beachrocks on the coast of Keos, Andros, and Paros Islands (Mendoni and Mourtzas 1990; Mourtzas 2010, 2018; Mourtzas and Kolaiti 1998, 2016; Kolaiti and Mourtzas 2020).

6.2 The rsl change curve for M–D–R in relation to the northern and central Cyclades

The rsl change history of the northern and central Cyclades during the last 6.3 ka, the periods of rsl stability, along with the corresponding periods of rsl stability for M–D–R, the estimated duration of each, and the interpolated periods of rsl change, are illustrated in Fig. 13. The curve of the rsl change represents the average rate of the rsl rise during the Late Holocene for the northern and central Cyclades.

The data indicate a coherent pattern of rsl rise at an average rate of 0.76 mm/year since the Late Neolithic (ca. 4300 BC), a period when the sea level was identified at 4.80 ± 0.10 m bmsl. The average rsl rise rate between sea-level stands I and II is 0.5 mm/year, while a significant acceleration is observed with estimated rates 3.70 mm/year between sea levels II and III, 1 mm/yr between III and IV, 2.77 mm/yr between IV and V, and an extremely high rate of 6.15 mm/year from the late nineteenth century to the present day. Moreover, by comparing the rsl change curve based on our observations with the predicted sea-level curve resulting

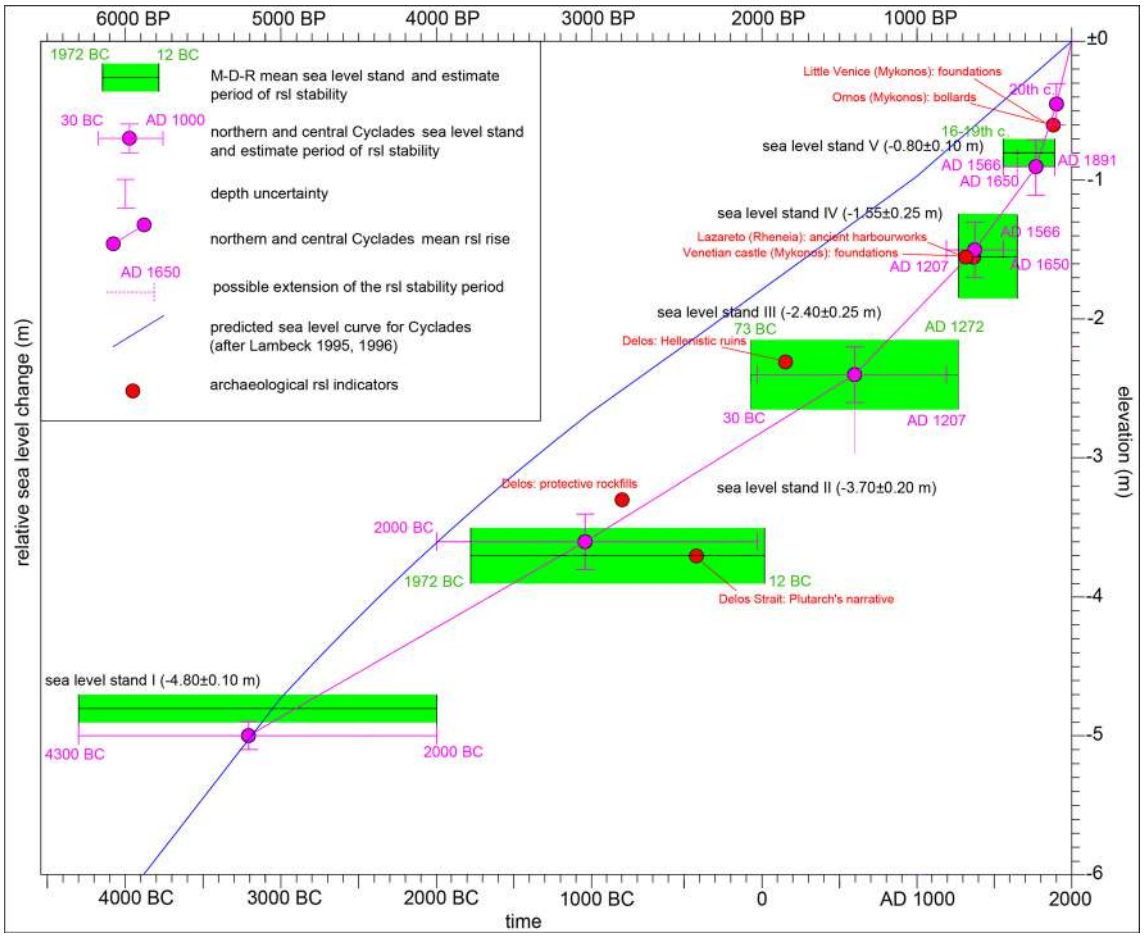

Fig. 13 The rsl curve for the island group of Mykonos-Delos-Rheneia (M–D–R) during the last 6300 years with respect to the relative sea level (rsl) curve of the northern and central Cyclades (after Kolaiti and Mourtzas 2020)

from the glacio-hydro-isostatic model for the Cyclades since 6 ka BP (Lambeck 1995, 1996; Lambeck and Purcell 2005), we extract a remarkable tectonic component, ranging from 1 to 1.20 m for sea levels II, III, and IV to 0.55 m for sea level V. These values, however, seem to be underestimated when compared with curves for Cyclades provided by other models, such as those detailed in Kolaiti and Mourtzas (2020), who, in an attempt to approach the geodynamic setting of the northern and central Cyclades, attributed the inferred long periods of rsl stability to long periods of tectonic quiescence, interrupted by strong deformation events that resulted in abrupt changes in the sea level.

6.3 M–D–R beachrocks

In this study, we attempted to reconstruct the rsl changes along the coast of M–D–R in relation to those of the central and northern Cyclades, not only as deduced from all the available geomorphological and archaeological rsl markers, but also following a specific method of approach to the beachrocks as indicators of the former sea levels. A different approach was followed by Desruelles et al. (2009) in their study of the M–D–R beachrocks, so far considered a 'standard' method for the Aegean and other beachrocks (see Vacchi 2012; Mauz et al. 2015). The main difference lies in their assumption that the cement throughout the full width of a beachrock slab (landward end-seaward end) represents an intertidal diagenetic environment. In our approach, we accept that the formation environment also extends to the swash and backwash zone and even occasionally to the spray zone (Pirazzoli 2001), thus ranging from slightly subtidal to supratidal, and only the seaward end of a beachrock slab represents the intertidal zone. This is further supported by the conclusion of Bernier and Dalongeville (1996) that diagenesis is similar in both the intertidal and the swash and backwash zones; hence, the results regarding the beachrock cement are indistinguishable. Through this prism, the method employed by Desruelles et al. (2009) entails a paradox. They accept that, for the same beachrock slab, the back-end (landward)

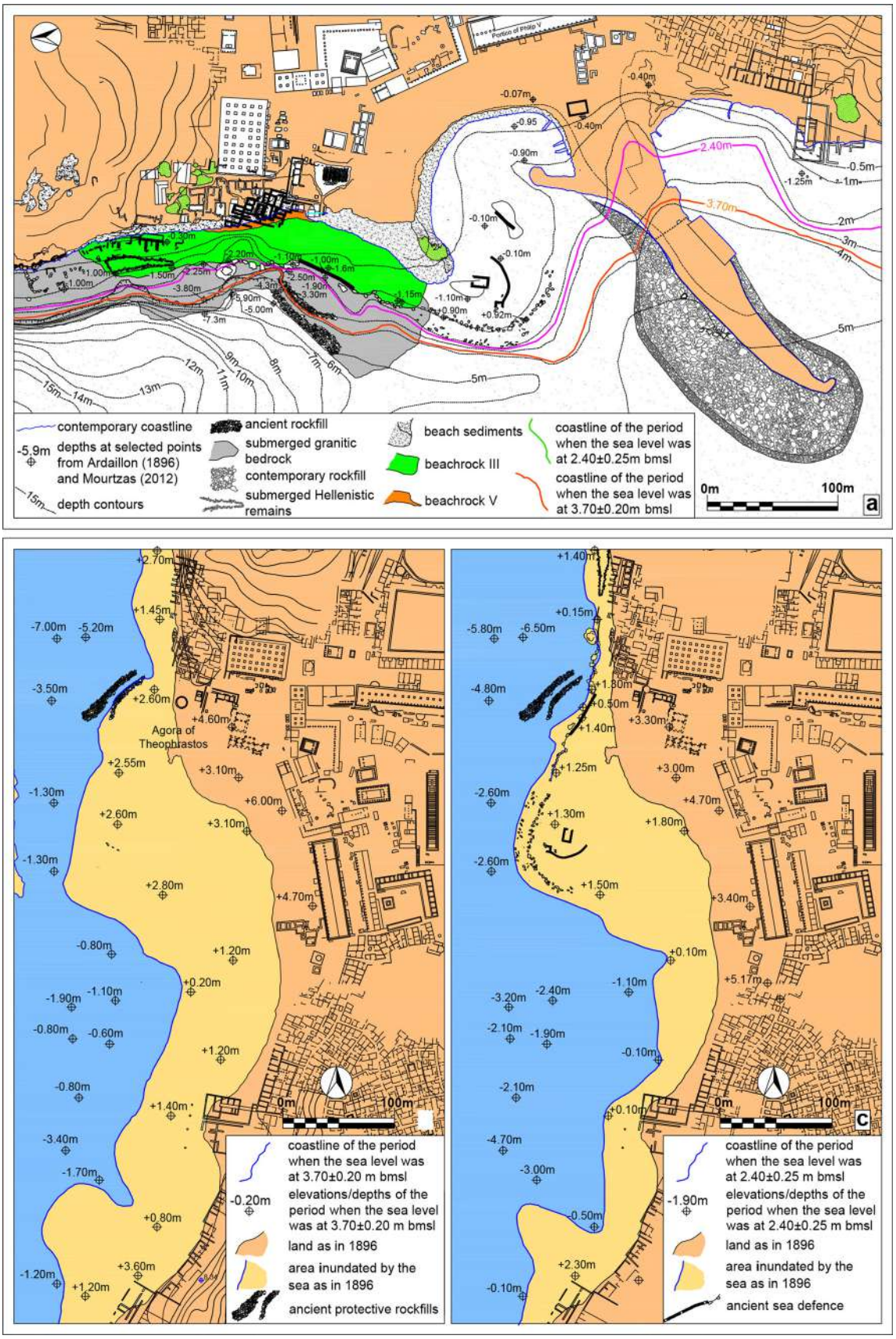
contemporary coastline
-5.9m depths at selected points from Ardaillon (1896) and Mourtzas (2012)
15m depth contours
ancient rockfill
submerged granitic bedrock
contemporary rockfill
submerged Hellenistic remains
beach sediments
beachrock III
beachrock V
coastline of the period when the sea level was at 2.40±0.25m bmsl
coastline of the period when the sea level was at 3.70±0.20m bmsl
0m
100m
a
Agora of Theophrastos
coastline of the period when the sea level was at 3.70±0.20 m bmsl
-0.20m elevations/depths of the period when the sea level was at 3.70±0.20 m bmsl
land as in 1896
area inundated by the sea as in 1896
ancient protective rockfills
coastline of the period when the sea level was at 2.40±0.25 m bmsl
-1.90m elevations/depths of the period when the sea level was at 2.40±0.25 m bmsl
land as in 1896
area inundated by the sea as in 1896
ancient sea defence
c

◂**Fig. 14** **a** The seafront of the ancient city of Delos. The coastlines during the historical period when the sea level was at 3.70 ± 0.20 m bmsl and 2.40 ± 0.25 m bmsl are indicated. **b**, **c** Palaeogeographic reconstruction of the ancient Delos seafront when the sea level was at: **b** 3.70 ± 0.20 m bmsl and **c** 2.40 ± 0.25 m bmsl. The elevations/depths are based on Ardaillon (1896), recorded before the later human interventions that altered the coastal morphology of the coast, and Mourtzas (2012)

is theoretically the oldest, and the front-end (seaward) is the youngest, which essentially means that were formed in different periods, an argument they use to justify the heterogeneous radiocarbon chronologies obtained from the two ends of the same beachrock slab. However, for reconstructing the intertidal zone of a former sea level during which the beachrock was formed, they calculate the average elevation of the top of both beachrock ends, even though they suggest that they are of different age, assuming an uncertainty ± 0.50 m. From this, a second paradox arises: in a semi-submerged beachrock slab (landward end amsl, seaward end bmsl), the central axis of the reconstructed intertidal zone of a former sea level is located above the sea level. According to our approach, the seaward and deeper end of a beachrock slab is the oldest and the landward end is the youngest, since the latter is formed by a continuous sediment supply during a period of either rsl stability or a slight rise in sea level, during which this slab is formed. This conforms to the model of beachrock formation in an area subject to subsidence (Online Resource-Figs. B, C and D).

Only under two certain conditions would the assumptions made by Desruelles et al. (2009) be reasonable:

(a) The sea level should have been remained stable throughout the formation of each beachrock generation and the beachrock should have been cemented within an intertidal zone with a tidal range from 0.70 m to 1 m, according to the depths given in their study. However, in the microtidal environment of the central Aegean, the maximum tidal range is 0.28 m, the minimum 0.01 m, and the average 0.14 m (statistical data from the tide-gauge station of Syros, operated by the Hellenic Navy Hydrographic Service-HNHS since 1979, TSDB 1990–2012).
(b) Given the microtidal range, each beachrock generation should have been formed during a continuously rising sea level at rapid rates. However, Desruelles et al. (2009) suggest that the beachrocks are formed within the intertidal zone during stages of shoreline stabilization (both eustatic and tectonic). In addition, considering the radiometric ages and the depth measurements provided by Desruelles et al. (2009) for the three beachrock generations that they determined, the rates of the rsl rise should be: 0.54 mm/year for the earliest and deepest beachrock generation (− 3.60 ± 0.50 m), 1.90 mm/year for the intermediate beachrock generation (− 2.50 ± 0.50 m), and 1.60 mm/year for the youngest and shallowest generation (− 1.00 ± 0.50 m). In essence, this means that the coastal sediments should have gradually cemented strictly in the intertidal zone with an average tidal range 0.14 m, while the sea level would have risen at extremely high rates.

Both conditions imply that the section of the beachrock slab of a maximum thickness 1 m below its upper surface (Desruelles et al. 2009) would have formed within the subtidal zone. From the extensive list of Mauz et al. (2015), which includes some 50 research papers related to beachrocks all around the globe, it is deduced that all examined beachrocks are cemented in the intertidal and upper intertidal zone, while in only two locations is cementation in the supratidal zone suggested. There is no reference to beachrock cementation occurring at depths lower than the mean low tide and at elevations higher than the range of the swash and backwash zone and, in some cases, the spray zone (Vousdoukas et al. 2007; Mauz et al. 2015 and related references therein).

The thickness of a beachrock slab depends on the supply of sediment and the local hydrodynamic conditions (e.g., Ginsburg 1953; Shinn 1969; Chivas et al. 1986; Kelletat 1988, 2006; Gischler and Lomando 1997; Ramkumar et al. 2000; Vousdoukas et al. 2007). This accounts for the variation in thickness of the same beachrock generation from place to place and, therefore, the variation in depth of the top of the landward and seaward ends (Kolaiti 2019). The data presented in Table 1 clearly indicate that the depths of the base of the seaward end of each beachrock generation almost coincide, with small deviations (0.10–0.30 m), whereas those of the top of the seaward and landward ends exhibit a significant variance of up to 0.70 m. In addition, the thickness of beachrock generation I is 0.70 m, while generations II and III range from 0.10 m to 1.50 m, and generations IV and V from 0.10 m to 0.75 m. Therefore, when the depth of the top of the beachrock slab is measured according to Desruelles et al., these variations in thickness lead to high depth uncertainty.

The three sea-level stands suggested by Desruelles et al. (2009) were determined on the basis of a small sample size from only seven locations throughout M–D–R, which leads to a higher variability and margin of error. If the former sea levels were determined using the depth measurements of this study from 22 locations throughout M–D–R, but applying the method used by Desruelles et al. (average between ends), then we would have the following sea levels for each rsl stability phase: 0.90 ± 0.60 m instead of 1.00 ± 0.50 m bmsl for the first phase, 1.45 ± 0.70 m bmsl instead of 2.50 ± 0.50 m bmsl for the second phase, and 2.90 ± 0.70 m bmsl instead of 3.60 ± 0.50 m bmsl for the third phase.

6.4 Palaeogeographic reconstruction of the Delos Strait and the seafront of the ancient city

Utilising the geomorphological and archaeological indicators of the rsl change on the seafront of ancient Delos (Dûchene and Fraisse 2001; Dalongeville et al. 2007; Mourtzas 2012) and the soundings of Ardaillon (1896) acquired before the later significant changes in the coastal morphology, a palaeogeographic reconstruction of the coast was attempted (Fig. 14). Tracing the ancient coastlines and their displacement over the course of time is of great importance in rsl change studies, but for the 'sacred island' this acquires even greater interest: *"Delos has no walls to mark its boundaries, or gates and tombs to point to its entrance: the sea is the boundary and the harbours are the gates to the city of Delos*" (Zarmakoupi 2018, 38).

With a sea-level stand at 3.70 ± 0.20 m bmsl, the coast by the 'House on the Hill' was 60 m wider than at present, while the protective rockfills along it would have protruded about 0.40 m from the then sea level (Fig. 14a, b). The coast of the so-called 'sacred harbour' [or main harbour, as it is referred to by Zarmakoupi (2015, 2018)], was 200 m wider than the current coastal zone, while the cove currently being created there was land. The coast of the 'Commercial Quarter' to the south extended 80 m into the sea (Fig. 14b). After the Hellenistic period (ca. 30 BC), the sea level rose by 1.30 m to 2.40 ± 0.25 m bmsl and caused the flooding of the coast by the 'House on the Hill', which shrunk by about 40 m. At that time, new sea defence works (boulders, rockfill, and seawall) were made along the then shoreline for the protection of the coastal buildings (Fig. 14a, c). The coast of the so-called 'sacred harbour' significantly shrank by about 30 m, with the current cove still being land. The coast of the 'Commercial Quarter' shrank by half and was only 40 m wider than at present.

Of great interest for the navigation of the time and approach of ships to Delos is the palaeogeography of the strait between the western coast of Delos and the eastern coast of Little and Great Rheumatiaris, the rocky islets. The strait today has a width of 150 m at its narrowest parts, with its depth not exceeding 5 m (Fig. 15a). During the prehistoric period when the sea level was 4.80 ± 0.10 m bmsl, Little Rheumatiaris (the northernmost islet) was joined to Delos by a sandy isthmus some 50 m wide, while Great Rheumatiaris was separated from Delos by a narrow and shallow (depth ≤ 1.50 m) waterway (Fig. 15b). When the sea level rose to 3.70 ± 0.20 m during the Classical and Hellenistic periods, the strait between Delos and Little Rheumatiaris did not exceed 60 m in width and 2 m in depth, while between Delos and Great Rheumatiaris it was 100 m wide and 2–3 m deep (Fig. 15c). Although the current coastal configuration exposes the seafront of the ancient city to the prevailing northerly winds and strong waves (Fig. 15a, rose diagram), at that time, it obviously would have been sheltered, allowing ancient ships to approach and anchor, without the need for specific harbourworks (Fig. 15c) (Mourtzas 2012; Zarmakoupi 2018; Nakas 2020). The narrow strait widened and deepened after the Hellenistic period, when the sea level rose to 2.40 ± 0.25 m bmsl (Fig. 15d).

6.5 Nicias and the 'bridge of boats'

After the purification of Delos by the Athenians in the winter of 426/5 BC (e.g., Antoniadis 2019), the Delia were reorganised into a penteteris[1] (Thuc. 3.104). Towards the end of the fifth century BC, probably in 417 BC (e.g., Herbin 2018), and definitely after the Peace of Nicias in 421 BC, the Athenian politician and general Nicias led the festal embassy from Athens to Delos, acting as architheore. Plutarch (Nic. 3.5) narrates that Nicias *with his choir, sacrificial victims, and other equipment* did not land directly on Delos but *landed first on the neighbouring island of Rheneia. Then, with the bridge of boats ('ζεῦγμα') which he had brought along with him from Athens, where it had been made to measure and signally adorned with gildings and dyed stuffs and garlands and tapestries, he spanned during the night the strait between Rheneia and Delos, which is not wide. At break of day, he led his festal procession in honor of the god, and his choir arrayed in lavish splendor and singing as it marched, across the bridge to land.*[2]

Jebb (1880) rejected Plutarch's narrative, suggesting Mikros Rheumatiaris (Little Rheumatiaris Islet) as Nicias's landing-place, and estimated that a distance of about 150 yards (137.16 m) was bridged, without taking into consideration the then sea level. Négris (1904) excluded one single bridge connecting Rheneia and Delos and argued that the two sea channels, that is between Rheneia and Megalos Rheumatiaris and between the latter and Delos, were about 400 m wide, impossible to bridge in one night. For Négris, this could have been possible only if Nicias had landed in Megalos Rheumatiaris and bridged at least half the distance. A pioneer in the field of sea level changes, Négris reasoned that the sea level stand at the time of Nicias was at least 3 m lower than at the beginning of the twentieth century, and suggested that Nicias had to bridge a narrow (approx. 70 m) and shallow (3-4 m) sea channel. Later scholars (e.g. Crawford and Whitehead 1983; Dillon 1997; Emerson 1997; Wilson 2000; Evans 2010; Hubbart 2011; Athanassaki 2020-1)

[1] Penteteris ('πεντετηρίς'): a space of four years elapsed between each and the next succeeding festival, according to the ancient mode of reckoning (retrieved from: https://www.perseus.tufts.edu/, accessed 21 June 2023).

[2] The English translation of Sect. 3.5 of Plutarch's Lives (Life of Nicias) by Bernadotte Perrin (1916) and the Greek quotation were retrieved from: http://www.perseus.tufts.edu/, accessed 10 Dec 2022.

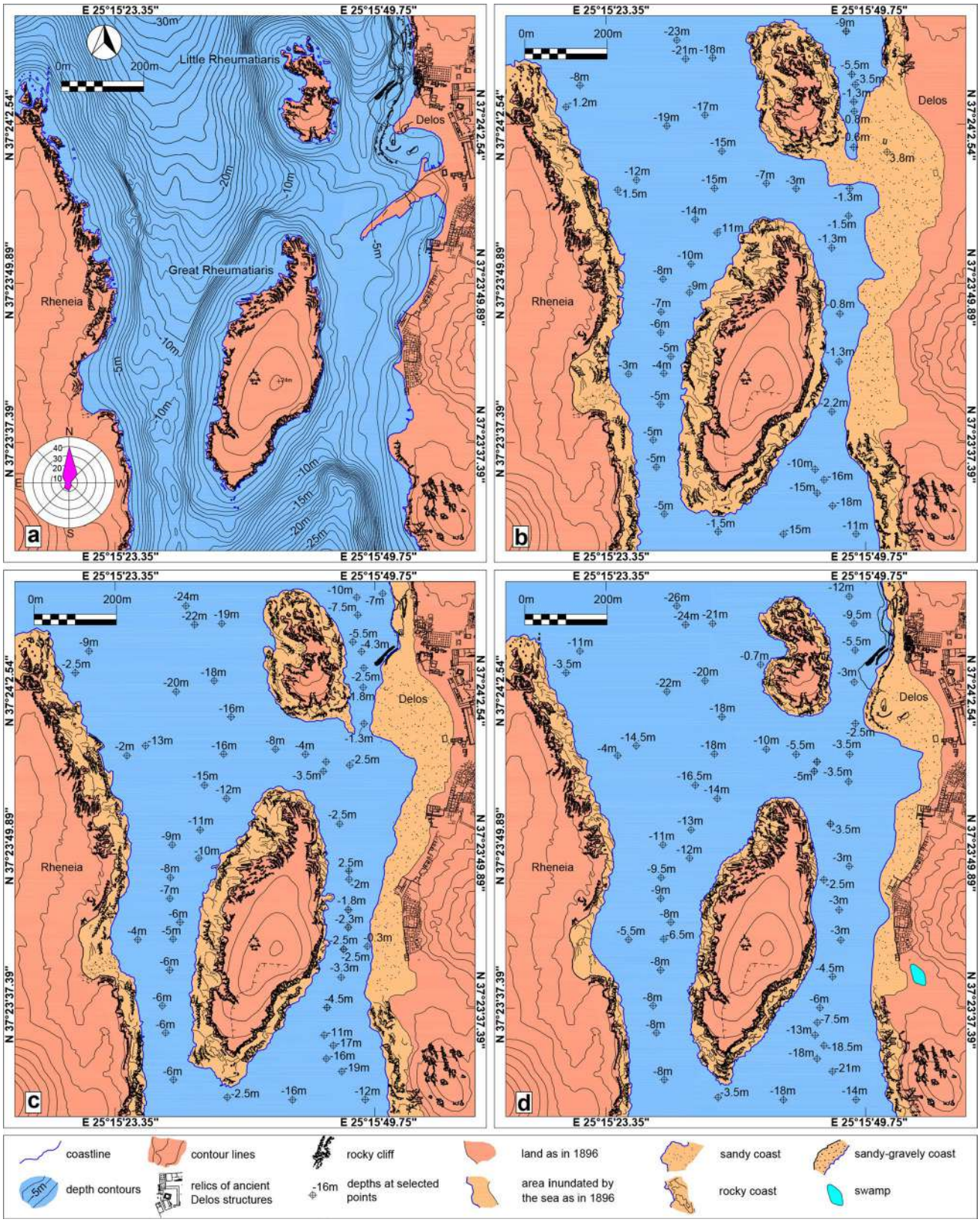

Fig. 15 **a** The Delos Strait as it now stands. The inset shows the wind rose diagram. **b**, **c**, **d** Palaeogeographic reconstruction of the Delos Strait when the sea level was at: **b** 4.80 ± 0.10 m bmsl, **c** 3.70 ± 0.20 m bmsl, and **d** 2.40 ± 0.25 m bmsl

reproduce Plutarch's narrative without questioning the feasibility of this project, given the particular seascape, shore accessibility, strait bathymetry, fleet availability, weather conditions, and particular time constraint for the installation of Nicias's 'bridge of boats': historiography from a geoarchaeological perspective.

Herodotus (7.33–7.36) provides technical details of how ships carrying bridges were used to bridge sea channels. At that time (fifth century BC), with the sea level 3.70 ± 0.20 m lower than at present, the strait between Delos and Rheneia had a breadth of about 750 m and a depth of 16 m in its central part (Fig. 15c). Of greater significance, perhaps, the SE coast of Rheneia was mainly rocky, with only one stretch of sand where Nicias's choir could land: just opposite the western coast of Great Rheumatiaris Islet, the eastern shore of which faced the coast of the Commercial Quarter, located some 500 m south of the sanctuary (Figs. 7e, 15c). As this does not match Plutarch's description of one unique bridge of boats connecting Rheneia directly with Delos nor the route of Nicias's procession to the sanctuary, the only reasonable hypothesis is that Plutarch implies the strait was spanned at some point between the Great (south) and Little (north) Rheumatiaris Islets (Fig. 15c).

If this hypothesis were true, to bridge the distance between Delos and Rheneia Islands (~750 m), Nicias would have had to accurately pre-dimension the bridge project, and have brought along some 95 triremes, with a gap between them estimated at 3 m, cables weighing at least 50 tn, proper anchors with long ropes to hold the ships in place until they were fastened to the cables (preventing displacement due to the currents and undercurrents caused by the prevailing north wind), and wooden logs for the bridge deck. Moreover, he would have had to provide appropriate bollards of some meters in diameter to fasten the cables on both shores, of which no remains have been mentioned so far. Considering that the date of the festival is assigned most probably to the month of Hieros, the second month in the Delian calendar (Arnold 1933) or alternatively to the month of Thargelion, the fifth month in the Delian calendar (Jebb 1880; Arnold 1933), which roughly correspond to January–February and April–May, respectively, the difficulties that may have been caused by winter winds or storms during the implementation of the project become obvious (Herodotus 7.34; Hammond and Roseman 1996).

Even if we assume that the weather conditions were favourable and accept that all the preparatory tasks were rightly accomplished, under no circumstances would it have been possible to set up such a bridge overnight, as Plutarch narrates, unless he exaggerates to overemphasise Nicias's capability. After all, Plutarch came along some five centuries later than Herodotus, as did Nicias himself, for that matter, and it is likely he rather wanted to convey Nicias's procession crossing the bridge as an impressive, wealthy, and glorious display for the Pan-Ionians standing on the opposite shore, communicating a political message from the leading state of the Delian league (Athanassaki 2020–1), than to deal with the practicalities of whether or not this project could actually have been carried out overnight. The most reasonable scenario is that Nicias *with his choir, sacrificial victims, and other equipment* (fn 1) landed on Little Rheumatiaris Islet, located opposite the waterfront of the ancient city. The distance between the shores of Delos and the islet would have been less than 60 m at the narrowest part (which is consistent with Plutarch's description of a narrow strait) and a sea depth not exceeding 2 m at the midpoint (Fig. 15c). This narrow waterway was fully protected against winds in all weathers. Nicias could have set up the bridge of boats in one night, placing about seven triremes in a series leaving a gap of some 3 m between them, without the need for a large amount of heavy materials and special equipment to construct the bridge for his procession, and more importantly without the risk of his project failing (Fig. 15c). Next morning, the amazed Pan-Ionians would have witnessed the spectacle of Nicias leading a magnificent and perhaps extravagant procession slowly across the bridge *signally adorned with gildings and dyed stuffs and garlands and tapestries* (fn 1), alighting upon the Sacred Island, and heading towards the temple of Apollo.

7 Conclusions

The rsl changes in M–D–R during the last 6300 years, substantiated by robust evidence of geomorphological and correlative archaeological sea-level markers, clearly point to a prominent marine transgression in the coastal area of the island group. This has significantly changed the position of the coastline and drastically affected both the coastal landscape and the interrelated seascape, featuring the interplay between human history and geography.

The indicators of the rsl change recorded and studied all along the coast of Mykonos, Delos, and Rheneia, provide a coherent pattern of rsl rise from the Late Neolithic period onward. Previous rsl reconstructions, which are also based on beachrocks as indicators of the rsl change, exhibit methodological gaps in the interpretation of the geomorphological indicator, insufficient field data and small sample size, and the sole use of absolute radiocarbon dating of carbonate cements uncorroborated by indirect dating of archaeological rsl markers. This has engendered underestimation of the number of former sea-level stands and their depth in relation to the mean sea level, as well as the chronological range of the rsl stability.

As accurate as possible an estimate of the number, depth and age of the Late Holocene sea-level stands is absolutely

essential for a palaeogeographic reconstruction of the numerous coastal archaeological sites in the Aegean that leads to a deeper understanding of the interaction between human and coastal environment during prehistoric times and historical antiquity.

Supplementary Information The online version contains supplementary material available at https://doi.org/10.1007/s42990-023-00104-4.

Acknowledgements The study of the sea-level changes in Cyclades began within the research project "Neotectonic deformations of the Aegean islands during the Upper Holocene and their impact on archaeological sites and monuments", directed by the late Professor Paul Marinos, National Technical University of Athens, and funded by the General Secretary of Research and Technology of the Hellenic Ministry of Industry (1991-1993). We would like to thank the former KA EPCA (now the Ephorate of Antiquities of the Cyclades), and especially the former Director, Fotini Zafeiropoulou, for her permission and support during the surveys and the interpretation of field data. We are grateful to Dr Vyron Antoniadis (Senior Researcher, Institute of Historical Research, National Hellenic Research Foundation) for a discussion we had on the section "Nicias and the bridge of boats". Three anonymous referees made important contributions on an earlier draft of this paper. Finally, we would like to thank Mr. Stephen John Taylor (TES) for his invaluable assistance in editing the English text.

Data availability The authors declare that the data supporting the findings of this study are available within the paper and its supplementary information file.

Declarations

Conflict of interest On behalf of all authors, the corresponding author states that there is no conflict of interest.

References

Alexouli-Livaditi A, Livaditis G (2004) The morphology of the coasts of the island of Andros. Retrieved from: https://docplayer.gr/39456304, accessed 5 Apr 2021

Altherr R, Kreuzer H, Wendt I, Lenz H, Wagner GA, Keller J, Harre W, Hohndorf A (1982) A Late Oligocene/Early Miocene high temperature belt in the anti-cycladic crystalline complex (SE Pelagonian, Greece). Geol Jahrb 23:97–164

Antonioli F, Anzidei M, Lambeck K, Auriemma R, Gaddie D, Furlani S, Orru P, Solinas S, Gaspari A, Karinja S, Kovacic V, Surace K (2007) Sea-level change during the Holocene in Sardinia and in the northeastern Adriatic (central Mediterranean Sea) from archaeological and geomorphological data. Quatern Sci Rev 26:2463–2486

Anzidei M, Antonioli F, Benini A, Gervasi A, Guerra I (2013) Evidence of vertical tectonic uplift at Briatico (Calabria, Italy) inferred from Roman age maritime archaeological indicators. Quatern Int 288:158–167

Ardaillon E (1896) Rapport sur les fouilles du port de Délos. BCH 20:428–445

Arnold IR (1933) Local festivals at Delos. Am J Archaeol 37(3):452–458

Athanassaki L (2020–21) Ritual and politics, individual and community in Plutarch's works: the life of Nicias as a test-case. Αριάδνη/Ariadne 27 (2020–21), 131–147

Auriemma R, Solinas E (2009) Archaeological remains as sea level change markers: a review. Quatern Int 26:134–146

Avcioğlu M, Yiğitbaş E, Erginal AE (2016) Beachrock formation on the coast of Gökçeada Island and its relation to the active tectonics of the region, northern Aegean Sea, Turkey. Quatern Int 401:141–152

Avigad D, Garfunkel Z (1991) Uplift and exhumation of high-pressure metamorphic terranes: the example of the Cycladic blueschists belt (Aegean Sea). Tectonophysics 188:357–372

Avigad D, Baer G, Heimann A (1998) Block rotations and continental extension in the Central Aegean Sea: paleomagnetic and structural evidence from Tinos and Mykonos. Earth Planet Sci Lett 157:23–40

Benjamin J, Rovere A, Fontana A, Furlani S, Vacchi M, Inglis RH, Galili E, Antonioli F, Sivan D, Miko S, Mourtzas N, Felja I, Meredith-Williams M, Goodman-Tchernov B, Kolaiti E, Anzidei M, Gehrels R (2017) Late Quaternary sea-level changes and early human societies in the central and eastern Mediterranean Basin: an interdisciplinary review. Quatern Int 449:29–57

Bernier P, Dalongeville R (1988) Incidence de l'activité biologique sur la cimentation des sédiments littoraux actuels. L'exemple des îles de Délos et de Rhénée (Cyclades, Greece). Comptes Rendus De Academie Des Science 307:1901–1907

Bernier P, Dalongeville R (1996) Mediterranean coastal changes recorded in beachrock cementation. Zeit. Geomorphol. NF, Suppl.-Bd, 102:185–198

Bernier P, Guidi BJ, Bottcher EM (1997) Coastal progradation and very early diagenesis of ultramafic sands as a result of rubble discharge from asbestos excavations (northern Corsica, western Mediterranean). Mar Geol 144:163–175

Blake MC, Bonneau M, Geyssant J, Kienast JR, Lepvrier C, Maluski H, Papanikolaou D (1981) A geological reconnaissance of the Cyclacic blueschist belt. Greece Bull Geol Soc Am 92:247–254

Bohnhoff M, Rische M, Meier T, Becker D, Stavrakakis G, Harjes H-P (2006) Microseismic activity in the Hellenic Volcanic Arc, Greece, with emphasis on the seismotectonic setting in the Santorini-Amorgos zone. Tectonophysics 423:17–33

Brichau S, Ring U, Carter A, Bolhar R, Monié P, Stockli D, Brunel M (2008) Timing, slip rate, displacement and cooling history of the Mykonos detachment footwall, Cyclades, Greece, and implications for the opening of the Aegean Sea basin. J Geol Soc Lond 165:263–277

Bröcker M, Franz L (2005) P-T conditions and timing of metamorphism at the base of the Cycladic blueschist Unit, Greece, The Panormos window on Tinos re-visited. N Jb Mineral (abh) 181:91–93

Bruneau P, Ducat J (2005) Guide de Delos, Sites et Monuments 1, 4th edition, Athens and Paris

Cayeux L (1907) Fixitè du niveau de la Mèditerranèe. Annales De Gèographie 16:97–116

Chivas A, Chappell J, Polach H, Pillans B, Flood P (1986) Radiocarbon evidence for the timing and rate of island development, beach-rock formation and hosphatization at Lady Elliot Island, Queensland, Australia. Mar Geol 69:273–287

Crawford HM, Whitehead D (1983) Archaic and Classical Greece: a selection of ancient sources in translation. Cambridge University Press, Cambridge

Dalongeville P, Desruelles S, Fouache É, Hasenohr C, Pavlopoulos K (2007) Hausse relative du niveau marin à Délos (Cyclades, Grèce): rythme et effets sur les paysages littoraux de la ville hellénistique. Méditerranée 108:17–28

Desruelles S, Fouache É, Pavlopoulos K, Dalongeville R, Peulvast J.-P., Coquinot Y, Potdevin J.-L. (2004) Beachrocks et variations récentes de la ligne de rivage en Mer Egée dans l'ensemble Insulaire Mykonos-Délos-Rhénée (Cyclades, Grèce). Géomorphologie: relief, processus, environnement 10(1):5–17

Desruelles S, Fouache É, Dalongeville R, Pavlopoulos K, Peulvast J-P, Coquinot Y, Potdevin J-L, Hasenohr Cl, Brunet M, Mathieu R, Nicot É (2007) Sea-level changes and shoreline reconstruction in the ancient city of Delos (Cyclades, Greece). Geodin Acta 20(4):231–239

Desruelles S, Fouache É, Çiner A, Dalongeville R, Pavlopoulos K, Kosun E, Coquinot Y, Potdevin J-L (2009) Beachrocks and sea level changes since Middle Holocene: Comparison between the Insular Group of Mykonos-Delos-Rhenia (Cyclades, Greece) and the southern coast of Turkey. Global Planet Change 66(1):19–33

Dillon M (1997) Pilgrims and pilgrimage in ancient Greece. Routledge

Dûchene H, Fraisse P (2001) Le paysage portuaire de la Délos antique: recherches sur les installations maritimes, commerciales et urbaines du littoral délien. Exploration Archéologique de Délos, fasc. 39, Ecole Française d'Athènes

Durr S, Altherr R (1979) Existence des klippes d'une nappe composite néogène dans l'ile de Mykonos, (Cyclades, Greece). Rapports De La Commission Internationale De La Mer Méditerranée, Monaco 25(26):33–34

Efa (2016) Guide de Délos, 4th ed. revised 30.1.2018, retrieved from: https://www.efa.gr/, accessed 7 Feb 2023

Emerson M (1997) Greek sanctuaries and temple architecture: an introduction. Bloomsbury

Engdahl E, Van der Hilst R, Buland R (1998) Global telesismic earthquake relocation with improved travel times and procedures for depth determination. Bull Seismol Soc Am 88:722–743

Erginal AE, Öztürk B (2012) Formation environment of the Kumlimani beachrock (Gelibolu Peninsula). Turkish Geogr Rev 57:87–93

Evans N (2010) Civic Rites, Democracy and Religion in ancient Athens. University of California Press

Facorellis G, Maniatis I (2002) Radiocarbon dating of the Neolithic settlement of Ftelia on Mykonos: calculation of the marine reservoir effect in The Cyclades. In: Sampson A (Ed) The Neolithic settlement at Ftelia, Mykonos, Department of Mediterranean Studies, Rhodes, 309–315

Faure M, Bonneau M, Pons J (1991) Ductile deformation and syntectonic granite emplacement during the late Miocene extension of the Aegean (Greece). Bull Soc Géol France 162:3–12

Flemming NC, Czartoryska NMG, Hunter PM (1973) Archaeological evidence for eustatic and tectonic components of relative sea level change in the South Aegean. In: Blackman DJ (Ed) Marine archaeology, colston papers, 23, 1–66

Fouache É, Desruelles S, Pavlopoulos K, Dalongeville R, Coquinot Y, Peulvast J-P, Potdevin J-L (2005) Beachrocks as indicators of Late Holocene sea level rise in Mykonos, Delos and Rhenia Islands (Cyclades, Greece). Zeitschrift Für Geomorphologie Suppl 137:37–43

Gifford JA (1995) The physical geology of the western Messara and Kommos. In: Shaw JW, Shaw MC (eds) Kommos I: the Kommos Region and Houses of the Minoan Town. Princeton University Press, NJ, pp 30–90

Ginsburg NR (1953) Beach rock in south Florida. J Sediment Petrol 23:85–92

Gischler E, Lomando AJ (1997) Holocene cemented beach deposits in Belize. Sed Geol 110(3–4):277–297

Hadjidakis PJ (2003) Delos. Olkos

Hammond NGL, Roseman LJ (1996) The construction of Xerxes' bridge over the hellespont. J Hellenic Studies 116:88–107. https://doi.org/10.2307/631957

Hanor SJ (1978) Precipitation of beachrock cements: mixing of marine and meteoric waters vs CO_2-degassing. J Sediment Petrol 48:489–501

Heckel PH (1983) Diagenetic model for carbonate rocks in Midcontinent Pennsylvanian eustatic cyclothems. J Sediment Petrolol Tulsa 53(3):733–759

Herbin F (2018) Votive and honorific monument offering practice(s) in Delos: evolution of a social practice in Apollo's sanctuary from archaic times to the Roman era. In: Angliker E, Tully J (Eds) Cycladic archaeology and research: new approaches and discoveries, pp 261–278

HNHS-Hellenic Navy Hydrographic Service (2015) Statistical data on sea level from Greek ports, 2nd revised edition

Hopley D (1986) Beachrock as a sea-level indicator. In: Van de Plassche O (Ed) Sea-level research: a manual for the collection and evaluation of data, Galliard Printers, Great Yarmouth, pp 157–173

Hubbart Th (2011) The dissemination of Pindar's non-epinician choral lyric. In: Athanassaki L, Bowie E (Eds) Archaic and classical choral song: performance, politics and dissemination, Walter de Gruyter, pp 347-364

Hughen KA, Baillie MGL, Bard E et al (2004) MARINE04 marine radiocarbon age calibration 26–0 ka BP. Radiocarbon 46:1059–1086

IGME (2004) Geological Map of Greece, 1:50000: Mykonos Island-Rinia Island Sheet. Institute of Geology and Mineral Exploration

Jebb RC (1880) Delos. J Hellenic Stud 1:7–62. https://doi.org/10.2307/623613

Jolivet L, Lecomte E, Huet B, Denèle Y, Lacombe O, Labrousse L, Le Pourhiet L, Mehl C (2010) The North Cycladic detachment system. Earth Planet Sci Lett 289:87–104

Jolivet L, Arbaret L, Le Pourhiet L, Cheval-Garabédian F, Roche V, Rabillard A, Labrousse L (2021) Interactions of plutons and detachments: a comparison of Aegean and Tyrrhenian granitoids. Solid Earth 12(6):1357–1388

Kahle H-G, Straub C, Reilinger R, McClusky S, King R, Hurst K, Veis G, Kastens K, Cross P (1998) The strain rate field in the eastern Mediterranean region, estimated by repeated GPS measurements. Tectonophysics 294:237–252

Karadima N-K (2013) The origin of barite minelarization on the Mykonos granite. Graduation thesis, Department of Geology, University of Patras

Karkani A, Evelpidou N, Vacchi M, Morhange Ch, Tsukamoto S, Frechen M, Maroukian H (2017) Naxos-Paros Tracking shoreline evolution in central Cyclades (Greece) using beachrocks. Mar Geol 388:25–37

Keiter M, Piepjohn K, Ballhaus C, Lagos M, Bode M (2004) Structural development of high-pressure metamorphic rocks on Syros island (Cyclades, Greece). J Struct Geol 26:1433–1445

Kelletat D (1988) Zonality of modern coastal processes and sea-level indicators. Palaeogeogr Palaeoclimatol Palaeoecol 68(2–4):219–230

Kelletat D (2006) Beachrock as sea-level indicator? Remarks from a geomorphological point of view. J Coastal Res 22(6):1555–1564

Kizildağ N, Özdaş H (2021) Relative sea-level changes along the Fethiye coast (SW Turkey) based on recent archaeological data. Geoarchaeology 36:474–489

Kolaiti E (2019) Changes in the anthropogenic environment along the eastern coast of the Peloponnese on the basis of archaeological and morphological indicators of the Late Holocene relative sea level changes. Proposing a geoarchaeological method of approach. PhD Thesis, University of the Peloponnese, Kalamata. http://www.didaktorika.gr/eadd/handle/10442/44943. Accessed 17 Feb 2023

Kolaiti E, Mourtzas N (2020) New insights on the relative sea level changes during the Late Holocene along the coast of Paros Island and the northern Cyclades (Greece). Annal Geophys 63(6):OC669, https://doi.org/10.4401/ag-8504

Kolaiti E, Papadopoulos AG, Morhange C, Vacchi M, Triantafyllou I, Mourtzas ND (2017) Palaeoenvironmental evolution of the ancient harbor of Lechaion (Corinth Gulf, Greece): Were changes

driven by human impacts and gradual coastal processes or catastrophic tsunamis? Mar Geol 392:105–121
Konioti M (2019) The castle of Mykonos town. In: The settlement of Kastro in Mykonos town, Municipality of Mykonos, 15–17, retrieved from: https://issuu.com/pelpal/, accessed 11 Apr 2021
Kreemer C, Chamot-Rooke N (2004) Contemporary kinematics of the southern Aegean and the Mediterranean Ridge. Geophys J Int 157(3):1377–1392
Lambeck K (1995) Late Pleistocene and Holocene sea-level change in Greece and south-western Turkey: a separation of eustatic, isostatic and tectonic contributions. Geophys J Int 122:1022–1044
Lambeck K (1996) Sea-level changes and shoreline evolution in Aegean Sea since Upper Paleolithic time. Antiquity 70:588–611
Lambeck K, Purcell A (2005) Sea-level change in the Mediterranean Sea since the LGM: model predictions for tectonically stable areas. Quatern Sci Rev 24:1969–1988
Lambeck K, Anzidei M, Antonioli F, Benini A, Esposito A (2004) Sea level in Roman time in the Central Mediterranean and implications for recent change. Earth Planetary Sci Lett 224:563–575
Lecomte E, Jolivet L, Lacombe O, Denèle Y, Labrousse L, Le Pourhiet L (2010) Geometry and kinematics of a low-angle normal fault on Mykonos island (Cyclades, Greece): evidence for slip at shallow dip. Tectonics 29:TC5012. https://doi.org/10.1029/2009TC002564
Lee J, Lister GS (1992) Late Miocene ductile extension and detachment faulting, Mykonos, Greece. Geology 20:121–124
Le Pichon X, Chamot-Rooke N, Lallemant S (1995) Geodetic determination of the kinematics of central Greece with respect to Europe: implications for eastern Mediterranean tectonics. J Geophys Res 100:12675–12690
Longman MW (1980) Carbonate diagenetic textures from near-surface diagenetic environments. AAPG Bull 64:461–487
Lucas I (1999) Le pluton de Mykonos–Delos–Rhenee (Cyclades, Grèce): un exemple de mise en place synchrone de l'extension crustale. PhD Thesis, Université d'Orléans, Orléans
Lykousis V (2009) Sea-level changes and shelf break prograding sequences during the last 400 ka in the Aegean margins: subsidence rates and palaeogeographic implications. Cont Shelf Res 29(16):2037–2044
Maluski H, Bonneau M, Kienast JR (1987) Dating the metamorphic events in the Cycladic area: 39Ar/40Ar data from metamorphic rocks of the island of Syros (Greece). Bull Soc Géol Fr 8:833–842
Mauz B, Vacchi M, Green A, Hoffmann G, Cooper A (2015) Beachrock: a tool for reconstructing relative sea level in the far-field. Mar Geol 362:1–16
Mendoni LG, Mourtzas ND (1990) An archaeological approach to coastal sites. The example of the ancient harbor of Karthaia. Proceedings of Triemero Aigaiou, 21–23 December 1989, Philologikos Syllogos Parnassos (Athens, Greece), Parnassos Journal, vol. AB', 387–403
Meyers JH (1987) Marine vadose beachrock cementation by cryptocrystalline magnesian calcite, Maui, Hawaii. J Sediment Petrol 57:558–570
Moore CH (1973) Intertidal carbonate cementation in Grand Cayman, West Indies. J Sediment Petrol 43:591–602
Mourtzas N (2007) Ancient harbour installations on the coast of Palaeopolis. In: Palaiokrassa-Kopitsa L (Ed) Palaeopoli of Andros: twenty years of archaeological research, pp 104–108
Mourtzas ND (2010) Sea level changes along the coasts of Kea island and palaeogeographical coastal reconstruction of archaeological sites. Bull Geol Soc Greece 43(1):453–463
Mourtzas ND (2012) A palaeogeographic reconstruction of the seafront of the ancient city of Delos in relation to Upper Holocene sea level changes in the central Cyclades. Quatern Int 250:3–18
Mourtzas N (2018) Palaeogeographic reconstruction of the coast of ancient Andros. In: Palaiokrassa-Kopitsa L (Ed) Palaiopolis, Andros: Thirty years of excavation research, Kaireıos Library, Andros, pp 56–66
Mourtzas ND, Kolaiti E (1998) Interaction of geological and archaeological factors: evolvement of the prehistoric and historical settlements and constructions in relation to the sea level changes on the coast of Keos Island. In: Mendoni LG, Mazarakis Ainian A (Eds) Kea-Kythnos: History and archaeology, Proc. Intern. Symp. Kea-Kythnos, 22–25 June 1994, Meletimata, 27:679–693
Mourtzas ND, Kolaiti E (2016) Holocene sea level changes and palaeogeographic reconstruction of the Ayia Irini prehistoric settlement (Keos Island, Cyclades archipelago, Greece). In: Ghilardi M (Ed) Géoarchéologie des îles de Méditerranée / Geoarchaeology of the Mediterranean Islands. CNRS Éditions
Mourtzas ND, Kolaiti E, Anzidei M (2016) Vertical land movements and sea level changes along the coast of Crete (Greece) since Late Holocene. Quatern Int 401:43–70
Nakas ID (2020) Ships and harbours of the Hellenistic and Roman Mediterranean: a new approach. Maritime Archaeology Graduate Symposium 2020, Honor Frost Foundation, 22–23 February 2020, Nicosia. Short Report Series, 1–25. https://doi.org/10.33583/mags2020.06
Négris Ph (1904) Vestiges antiques submergés. Mitteilungen Archäologischen Instituts-Athenische Abteilung 29:340–363
Neumeier U (1999) Experimental modeling of beachrock cementation under microbial influence. Sed Geol 126:35–46
Neumeier U, Bernier P, Dalongeville R, Oberlin Ch (2000) Highlighting Holocene sea-level changes underlined by beachrock features and diagenesis: example from Damnoni (Crete). Geomorphologie: Relief Processus Environ 4:211–220
Okal EA, Synolakis CE, Uslu B, Kalligeris N, Voukouvalas E (2009) The 1956 earthquake and tsunami in Amorgos. Greece Geophys J Int 178(3):1533–1554
Papadopoulos GA, Pavlides SB (1992) The large 1956 earthquake in the South Aegean: macroseismic field configuration, faulting and neotectonics of Amorgos island. Earth Planet Sci Lett 113:383–396
Papageorgiou-Venetas A (1981) Délos: Recherches urbaines sur une ville antique. Deutscher Kunstverlag, Berlin
Papazachos BC, Karakostas VG, Papazachos CB, Scordilis EM (2000) The geometry of the Wadati-Benioff zone and lithospheric kinematics in the Hellenic arc. Tectonophysics 319:275–300
Paris J (1916) Contributions à l'étude des ports antiques du monde grec. Le Port De Délos BCH 40:5–73
Pelekis V (2019) The settlement and the house in Kastro. In: The settlement of Kastro in Mykonos town, Municipality of Mykonos, 13–15, retrieved from: https://issuu.com/pelpal/, accessed 11 Apr 2021
Pe-Piper G, Piper WJD, Matarangas D (2002) Regional implications of geochemistry and style of emplacement of Miocene I-type diorite and granite, Delos, Cyclades, Greece. Lithos 60:47–66
Pirazzoli PA (2001) De l'interprétation de la cimentation dans un beachrock. Quelques remarques sur Les variations holocènes du niveau marin mises en évidence par les caractères de la diagenèse des beachrocks; exemple de Damnoni (Crete). Geomorphologie: relief, processus, environnement, 7(4):295
Pizarro O, Jakuba M, Flemming N, Sakellariou D, Henderson J, Johnson-Roberson M, Mahon I, Toohey L, Dansereau D, Lees C (2012) AUV-assisted Characterization of Beachrock Formations in Vatika Bay, Laconia, Greece and their Relevance to Local Sea Level Changes and Bronze Age Settlements. Poster presentation in Ocean Sciences 2012 Meeting, 20–24 February 2012, Salt Lake City, Utah, USA. 2012

Plomaritis T (199) Morphology and Geochemistry of the Beachrocks of Sifnos (Greece). MSc Thesis, University of Southampton
Rabillard A, Jolivet L, Arbaret L, Bessière E, Laurent V, Menant A, Augier R, Beaudoin A (2018) Synextensional granitoids and detachment systems within Cycladic metamorphic core complexes (Aegean Sea, Greece): toward a regional tectonomagmatic model. Tectonics 37(8):2328–2362
Ramkumar M, Pattabhi Ramayya M, Gandhi MS (2000) Beachrock exposures at wave cut terraces of Modern Godavari delta: their genesis, diagenesis and indications on coastal submergence and sea-level rise. Indian J Marine Sci 29(3):219
Reimer PJ, McCormac FG (2002) Marine radiocarbon reservoir corrections for the Mediterranean and Aegean Seas. Radiocarbon 44(1):159–166
Reimer PJ, Bard E, Bayliss A et al (2013) IntCal13 and Marine13 radiocarbon age calibration curves 0–50,000 years cal BP. Radiocarbon 55(4):1869–1887
Sampson A (2018) The Neolithic Settlement at Ftelia, Mykonos. An intra-site analysis. In: Sampson A, Tsourouni T (Eds) Ftelia on Mykonos, Greece: Neolithic networks in the southern Aegean basin, University of the Aegean, Laboratory of Environmental Archaeology, II, Monograph Series, 7:1–14
Schmidt HA (2006) Regeneration on the sea front of Mykonos. Diploma Project, Faculty of Architectural Engineering, NTUA, retrieved from: http://courses.arch.ntua.gr/, accessed 15 May 2019
Scholle PA, Ulmer-Scholle DS (2003) A color guide to the petrography of carbonate rocks: grains, textures, porosity, diagenesis. American Association of Petroleum Geologists, Tulsa, Oklahoma
Shinn EA (1969) Submarine lithification of Holocene carbonate sediments in the Persian Gulf. Sedimentology 12:109–144
Skarpelis N (2002) Geodynamics and evolution of the Miocene mineralization in the Cycladic-Pelagonian Belt, Hellenides. Bull. Geol. Soc. Greece, XXXIV/6, 2191–2206
Strasser A, Davaud E, Jedoui Y (1989) Carbonate cements in Holocene beachrock: example from Bahiret el Biban, southeastern Tunisia. Sed Geol 62:89–100
Stuiver M, Reimer PJ, Reimer RW (2018) CALIB 7.1. http://calib.org. Accessed 6 June 2023
Taylor MCJ, Illing VL (1969) Holocene intertidal calcium carbonate cementation, Qatar, Persian Gulf. Sedimentology 12:69–107
Turner JR (2005) Beachrock. In: Schwartz ML (ed) Encyclopedia of coastal science. Kluwer Academic Publishers, The Netherlands, pp 183–186
Vacchi M (2012) Coastal geomorphology of Lesvos Island: Processes, late Quaternary evolution and the neotectonic implications. PhD Thesis in Earth Science, Dipartimento per lo Studio del Territorio e delle Sue Risorse, Università Degli Studi di Genova
Vacchi M, Ghilardi M, Spada G, Currás A, Robresco S (2017) New insights into the sea-level evolution in Corsica (NW Mediterranean) since the late Neolithic. J Archaeol Sci Rep 12:782–793
Vousdoukas M, Velegrakis A, Plomaritis TA (2007) Beachrock occurrence, characteristics, formation mechanisms and impacts. Earth Sci Rev 85:23–46
Webb GE, Jell JS, Baker JC (1999) Cryptic intertidal microbialites in beachrock, Heron Island, Great Barrier Reef: implications for the origin of microcrystalline beachrock cement. Sed Geol 126(1–4):317–334
Wilson P (2000) The Athenian Institution of the Khoregia: The Chorus, the City and the Stage. Cambridge University Press
YPPOA (Hellenic Ministry of Culture and Sports), 2020. Rhenia, the other Delos, retrieved from: https://www.culture.gov.gr/, accessed 5 Nov 2021
Zarmakoupi M (2015) Hellenistic & Roman Delos: the city & its emporion. Archaeol Rep 61:115–132
Zarmakoupi M (2018) The urban development of late Hellenistic Delos. In: Martin-McAuliffe SL, Millette DM (Eds) Ancient Urban Planning in the Mediterrannean: New Research Directions, Rutledge, 28–49
Zarmakoupi M, Athanasoula M (2017) The Delos Underwater Survey Project (2014–2016). Under the Mediterranean: 100 years on…The Honor Frost Foundation Conference of 'Mediterranean Maritime Archaeology'. Nicosia, 20–24 October 2017.
Zarmakoupi M, Athanasoula M (2018) Underwater archaeological investigation of the northeast side of Delos (Stadion District). In: Simosi A, Sotiriou S (Eds) Diving in the past: the underwater archaeological research 1976–2014, Hellenic Ministry of Culture, 91–10